Efficiency of sympagic-benthic coupling revealed by analyses of n-3 fatty acids, IP25 and other highly branched isoprenoids in two filter-feeding Arctic benthic molluscs: Mya truncata and Serripes groenlandicus

Rémi Amiraux, Philippe Archambault, Brivaela Moriceau, Mélanie Lemire, Marcel Babin, Laurent Memery, Guillaume Massé, Jean-Eric Tremblay

Efficiency of sympagic-benthic coupling revealed by analyses of n-3 fatty acids, IP_{25} and other highly branched isoprenoids in two filter-feeding Arctic benthic molluscs: *Mya truncata* and *Serripes groenlandicus*

Rémi Amiraux[a, b*], Philippe Archambault[a,c], Brivaela Moriceau[b], Mélanie Lemire[d], Marcel Babin[a], Laurent Memery[b], Guillaume Massé[a], Jean-Eric Tremblay[a]

[a] Takuvik International Research Laboratory, Québec Océan, Laval University (Canada) - CNRS, Département de biologie and Québec-Océan, Université Laval, Québec, Québec, Canada

[b] Laboratoire des Sciences de l'Environnement MARin (LEMAR), UMR 6539 CNRS/Ifremer/IRD/UBO, Institut Universitaire Européen de la Mer (IUEM), Technopôle Brest-Iroise, Plouzané, France

[c] ArcticNet, Québec Océan, Département de Biologie, Université Laval, Quebec, QC, Canada

[d] Axe santé des populations et pratiques optimales en santé, Centre de recherche du CHU de Québec, Université Laval, Québec, Canada

*Correspondence to: R. Amiraux (remi.amiraux@takuvik.ulaval.ca); Tel.: +1 418 440 3276

Abstract

The aim of this work was to determine the impact of sympagic (ice-associated) algal primary production on the quality of Arctic filter-feeding bivalves. For this purpose, we investigated the sea ice production of lipids (including omega−3 polyunsaturated fatty acids (n-3 PUFA) and highly branched isoprenoids (HBI)), as well as their subsequent incorporation into the truncate softshell clam (*Mya truncata*) and the Greenland cockle (*Serripes groenlandicus*) during the melting periods of two consecutive years in Baffin Bay. Lipid and primary production exhibited seasonal variability and overall contrasts between the two years as a result of distinct physical forcings and the ensuing biological responses. Whilst less productive in terms of total lipids or chlorophyll *a*, Spring 2016 was more productive than Spring 2015 for n-3 PUFA, which are essential for benthic fauna. The sea ice diatom HBI biomarker IP_{25} was quantified in sea ice from both years. Interestingly, such production was preceded by a production of the hitherto 'pelagic' biomarker, HBI III, in sea ice. In bivalves, HBI contents and correlations confirmed the tightness of the Arctic sympagic-benthic coupling and highlighted that *S. groenlandicus* can be used as a sentinel species for assessing the degree of this coupling. The confirmation that bivalves incorporate sea-ice derived HBI III and not only IP_{25}, may introduce uncertainties into the use of some HBI-based indices. Monitoring of the fatty acid contents of bivalves allowed identification of their spawning periods and suggests that *M. truncata* did not store enough n-3 PUFA to sustain its reproductive effort.

Keywords: Arctic shelves; Sympagic-benthic coupling; IP_{25}; HBI; n-3 PUFA; EPA; DHA; *Mya truncata*; *Serripes groenlandicus*; ice-derived HBI III;

1. Introduction

Arctic marine food webs are classically viewed as being supported by two ecologically distinct types of primary production effected in sequence by sympagic (ice-associated) algae and pelagic (water column) algae or phytoplankton (Gosselin et al., 1997; Horner and Schrader, 1982; Pabi et al., 2008; Wassmann et al., 2011). Among the essential organic molecules produced by algae, omega-3 polyunsaturated fatty acids (n-3 PUFA), such as eicosapentaenoic acid (EPA) 20:5(n-3) and docosahexaenoic acid (DHA) 22:6(n-3), are considered as highly relevant indicators of nutritional value for consumers (Hendriks et al., 2003). These specific lipids are produced almost exclusively by algae and are necessary for the whole food web, from primary consumers (e.g., bivalves) to top predators and even human populations. As algal species differ in their lipid production and more specifically in their PUFA contents (Leonardos and Lucas, 2000; Napolitano et al., 1990; Volkman et al., 1989), it is not surprising that EPA and DHA derive from different sources of primary production. Indeed, EPA is mostly produced by diatoms, a dominant taxon of both sympagic and pelagic algae (Kelly and Scheibling, 2012; Poulin et al., 2011; Viso and Marty, 1993), while DHA is associated with dinoflagellates, a mostly pelagic taxon (Kelly and Scheibling, 2012; Poulin et al., 2011; Søreide et al., 2008).

Sympagic and pelagic contributions to total primary production are highly variable depending on the season and the region, but it is generally admitted that sympagic algae contribute less than phytoplankton to annual primary production (Dupont, 2012; Fernández-Méndez et al., 2015). In contrast, sympagic primary production is recognized as an important contributor of carbon (C) exported towards the seafloor (Boetius et al., 2013; McMahon et al., 2006). This strong contribution results from the high sinking rates of ice-algal cells or aggregates (Boetius et al., 2013; Riebesell et al., 1991) and their good preservation during transit (Amiraux et al., 2017; Amiraux et al., 2020). In contrast, phytoplankton have a longer

76 residence time in the water column due to their slow sinking rates (van der Loeff et al., 2002),
77 which can lead to higher bacterial degradation and can reduce the quality of algal material
78 reaching the seafloor (Morata and Renaud, 2008; Roy et al., 2015). It is therefore not
79 surprising that the essential fatty acid content of this material is relatively high when it derives
80 from sea ice (Falk-Petersen et al., 1998; McMahon et al., 2006; Sun et al., 2009; Wang et al.,
81 2014). On this basis, sympagic algae are considered as a prime food source for benthic
82 consumers that depend on these fatty acids for growth and reproduction (Lovvorn et al., 2005;
83 McMahon et al., 2006; North et al., 2014).

84 Determining the impact of each primary production source on the quality of food for the
85 benthic community requires an estimation of their relative contributions. Several approaches
86 have been employed for estimating these contributions (e.g., stable isotopes and fatty acid
87 biomarkers; Gaillard et al., 2017; Gaillard et al., 2015). Among these, quantification of highly
88 branched isoprenoid (HBI) alkenes has provided robust estimates of the relative share of
89 different microalgal primary production sources in consumer biomass (Brown et al., 2017;
90 Brown and Belt, 2012). In recent years, the development of HBI-based proxies has
91 highlighted the relatively high source-specificity of a number of these molecules. Among
92 these, IP_{25} (Ice Proxy with 25 carbon atoms; Belt et al., 2007) is a mono-unsaturated C_{25} HBI
93 (**Fig. 1**) which seems to be produced exclusively by certain Arctic sympagic diatoms (e.g.,
94 *Pleurosigma stuxbergii* var. *rhomboides* (Cleve in Cleve & Grunow) Cleve, *Haslea kjellmanii*
95 (Cleve) Simonsen, *Haslea* spicula (Hickie) Lange-Bertalot; Brown et al., 2014c; Limoges et
96 al., 2018). A close structural analogue of IP_{25}, but with an additional double bond in its
97 structure, is known as HBI IIa (**Fig. 1**) and this co-occurs with IP_{25} in Arctic sea ice and
98 associated sediments. In a recent study, Belt et al. (2016) identified HBI IIa in the Southern
99 Ocean and showed it to be produced by the sympagic diatom *Berkeleya adeliensis* (Medelin).
100 The authors proposed the term $IPSO_{25}$ (ice proxy for the Southern Ocean with 25 carbon

atoms) for this biomarker, at least when detected in this ocean (Belt et al., 2016). Finally, a third (at least) HBI has been identified in several *Rhizosolenia* spp. isolated from polar and sub-polar locations (Belt et al., 2017) and has been linked with pelagic primary production under ice-free conditions in both the Arctic and the Antarctic (Belt, 2018; Belt et al., 2015; Collins et al., 2013; Massé et al., 2011). As a common constituent of marine settings (Belt et al., 2000), this tri-unsaturated HBI, sometimes referred to as HBI III (**Fig. 1**), has shown potential as a proxy of pelagic production for the spring marginal ice zone (MIZ) in polar seas (Belt et al., 2019; Collins et al., 2013; Köseoğlu et al., 2018; Smik et al., 2016a; Smik et al., 2016b). More recently, HBI III has also shown potential as a proxy for pelagic productivity associated with arctic sea fronts (Harning et al., 2020).

It is commonly accepted that a large proportion of the sympagic algal biomass released during sea ice melt, sinks to the seafloor, where it provides an important initial C and n-3 PUFA source for benthos growth and reproduction after the food limited winter (McMahon et al., 2006; North et al., 2014). However, to the best of our knowledge, no studies have jointly monitored the temporal evolution of primary production quality (n-3 PUFA) and source (HBIs) in sea ice and the benthic filter-feeders underneath. In order to enhance our understanding of pelagic-benthic coupling in the Arctic, the present study monitored the temporal evolution of n-3 PUFAs and HBIs in sea ice and two benthic filter-feeder bivalve molluscs (*Mya truncata* and *Serripes groenlandicus*) during two melting periods in southwest Baffin Bay. Our objectives were: (i) to determine the seasonal and interannual variability of sea ice high-quality lipid production in sea ice, (ii) to determine the seasonal and interannual enrichment of these lipids in the two bivalve species and (iii) to confirm the use of *M. truncata* and *S. groenlandicus* as indicators of the tightness of pelago-benthic coupling. This study will enhance our understanding of the Arctic pelagic-benthic coupling, as well as

highlight the seasonal and annual influences of sea ice lipid production on the quality of bivalves and of their reproductive capacity.

2. Materials and Methods

2.1 Study site and sampling

Sampling was conducted in 2015 and 2016 at a landfast-ice station located near Qikiqtarjuaq Island (**Fig. 2**) in southwest Baffin Bay (Canadian Arctic) within the framework of the GreenEdge project. Sea ice sampling was conducted every 2-3 days from 24 April to 24 June 2015 and from 16 May to 08 July 2016 (67°28.766'N; 63°47.579'W; water column depth: 350 m; **Fig. 2).** Bivalves (mean wet mass ± SE= 53.3 ± 3.5 and 42.4 ± 3.0 g for the truncate softshell clam (*Mya truncata*) and the Greenland cockle (*Serripes groenlandicus*) respectively; **Table S1**), were collected every 2–3 weeks from 18 January to 11 June 2015 and from 07 January to 19 June 2016, by scuba diving, at the closest coastal area from the sea ice sampling location (ca. 7.5 km west; 67°29.07'N; 63°57.92'W; **Fig. 2**).

Sea ice, sampled using a Kovacs Mark V 14 cm diameter corer focusing on the bottommost three centimeters of the core, where the bulk of ice biota occur (Smith et al., 1990), was retained for subsequent analyses of particulate organic matter (POM). To compensate for the horizontal heterogeneity of ice-algal biomass, which is typical of sea ice (Gosselin et al., 1986), sections from three or four equivalent cores were pooled in isothermal containers for each sampling. Pooled sea-ice sections were then melted with 0.2 µm filtered seawater (FSW; 3 parts of FSW to 1 part of melted ice) to minimize osmotic stress on the microbial community during melting (Bates and Cota, 1986; Garrison and Buck, 1986) and subsequently filtered for the several analyses (i.e., lipids, Chl *a*; Sections 2.2–2.3). Sea ice core parameters (e.g., snow thickness, air temperature and photosynthetically active radiation (PAR) estimated at the bottom of sea ice) were collected during both 2015 and 2016 campaigns and have already been published elsewhere (Amiraux et al., 2019; Massicotte et

al., 2019; Oziel et al., 2019). Briefly, for each sampling date, 5–8 snow depth measurements were made with a ruler. Air temperature records were made with a meteorological station: an automated Meteo Mat equipped with temperature sensor (HC2S3; Campbell Scientific) sensor positioned near (< 100 m) the sea ice station. Photosynthetically active radiation (PAR) below the sea ice was estimated at 1.3 m using the multispectral data collected with a Compact – Optical Profiling System (C-OPS; version IcePRO; Biospherical instruments Inc.; Oziel et al., 2019). To reduce the effect of sea ice surface heterogeneity on irradiance measurements (e.g., Katlein et al., 2015), the vertical attenuation coefficients of PAR were calculated by fitting a single exponential function on PAR profiles between 10 and 50 m, then used to estimate PAR at 1.3 m (more details are given by Massicotte et al., 2018). Note that 1.3 m corresponds to the highest average ice thickness measured during the two field campaigns and therefore to the first measurement under the ice (122.1 and 129.9 cm in 2015 and 2016 respectively).

After collection, bivalve samples were kept frozen (< –20°C) at the shore laboratory, before further treatment at the university laboratory. At Université Laval, bivalve individuals were freeze-dried and subsequently crushed (with exception of the shell), homogenized and kept frozen (< –20°C) prior to analysis.

2.2 *Chlorophyll* a

At the shore laboratory and within 24 h of sampling, sea ice samples originating from the pooled ice cores melted in isothermal containers were filtered in duplicates for chlorophyll *a* (Chl *a*) analyses through Whatman GF/F glass fiber filters. The Chl *a* retained on the filters was measured using a TD-700 Turner Design fluorimeter, after 18–24 h extraction in 90% acetone at 4°C in the dark (Parsons et al., 1984). The fluorimeter was calibrated with commercially available Chl *a* (*Anacystis nidulans*, Sigma).

178 *2.3 Lipid analyses*
179
180 At the shore laboratory, sea ice samples originating from pooled ice cores in isothermal
181 containers were filtered in duplicate for lipid analyses through Whatman GF/F glass fiber
182 filters (porosity 0.7 µm, pre-combusted 4 h at 450°C) and stored at –20°C before further
183 treatment at the university laboratory. At Université Laval, extraction of lipids was carried out
184 in duplicate on the algal filters (ca. 50–2500 mL filtered) and on bivalves (ca. 0.5 g dry mass).
185 To enable HBI and fatty acid quantification, two or three internal standards were added to
186 each sample prior to extraction. For HBI quantification, 7-hexylnonadecane (7-HND; 0.01
187 µg) was added to sea ice samples, while 9-octylheptadecene (9-OHD; 0.02 µg) was added to
188 bivalve samples. For fatty acid quantification, 100 µg and 500 µg of 5β-cholanic acid were
189 added to sea ice and bivalve samples respectively. Samples were saponified (5% KOH; 90°C,
190 120 min; 4 mL) in a flask, then extracted three times with hexane to recover HBI fractions
191 and subsequently collected using open column silica chromatography (ca. 1 g silica; 6–7 mL
192 hexane; Belt et al., 2012). The remainder of the flask was acidified with HCl to pH 1 and
193 extracted again three times with hexane (6–7 mL hexane). The combined hexane extracts
194 were dried over anhydrous Na_2SO_4, filtered and concentrated to obtain the fatty acid fraction
195 and methylated for further detection by gas chromatography-mass spectrometry (GC-MS).
196 Analysis of lipids was carried out using GC–MS in selected ion monitoring (e.g., SIM, *m/z*
197 350 (IP_{25}), 348 (HBI IIa, b) and 346 (HBI III, IV); **Fig. 1**) mode using an Agilent 7890A
198 series gas chromatograph (DB_{5MS} fused silica column; 50 m x 0.25 mm i.d., 0.25 µm film
199 thickness) coupled to an Agilent 5975C mass spectrometric detector (Belt et al., 2012). HBIs
200 were identified by comparison of retention indices ($RI_{DB5\text{-}MS}$) and mass spectra to those of
201 authentic standards (Belt, 2018; Belt et al., 2000; Tesi et al., 2020; Tesi et al., 2017).
202 Quantification of HBIs was carried out by comparing mass spectral intensities of molecular
203 ions to that of the internal standard and normalizing for differences in mass spectral

fragmentation efficiency and volume/mass sampled. Fatty acid quantification was made in a similar manner to that of HBIs, although using different standards (Supelco® 37 Component FAME Mix, Supelco).

2.4 Statistical analyses

2.4.1 Sea ice

Principal Component analysis (PCA) biplots of the environmental variables was used to reduce the dimensionality of the dataset using the "FactoMineR" package (Pagès, 2004). Environmental variables used into the PCA were total fatty acid (TFA), polyunsaturated fatty acid (PUFA), air temperature, PAR, snow thickness and Chl *a*, to describe the 28 and 23 sea ice sampling dates from 2015 and 2016, respectively. Wilcoxon tests were performed to test the effect of year (fixed with two levels: 2015 and 2016) on sea ice fatty acid (TFA, monounsaturated fatty acid (MUFA), PUFA, saturated fatty acid (SFA)) and HBI (IP_{25}, HBI IIa, IIb, III and IV) contents. Spearman's rank order correlation (r) was used to infer the strength of associations between HBI variables and correlation significance was determined at *p-value* $<$ 0.01.

2.4.2 Bivalves

Non-metric multidimensional scaling (nMDS), based on the Euclidean distance on normalized lipid data, was employed to graphically represent the position of the 75 bivalve specimens on the ordination diagram.

3. Results

3.1 Sea ice

On average, Chl *a* concentration in sea ice was ca. 6 times higher in 2015 than in 2016 (mean ± SE = 646.7 ± 69.4 µg L^{-1} and 119.8 ± 17.4 µg L^{-1}, respectively; **Fig. 3**). A unique Chl *a* peak in production was observed in 2015 (May 31st; 1661.8 µg L^{-1}) while two peaks were

observed in 2016 (317.3 and 306.9 µg L^{-1} on June 1st and 13rd respectively). TFA content in sea ice was ca. 5 times higher in 2015 than 2016 (mean ± SE = 57.9 ± 14.0 mg L^{-1} and 11.0 ± 2.7 mg L^{-1}, respectively; **Fig. 3**, **Table 1**). In 2015, the TFA maximum was observed on 15 June (332.0 mg L^{-1}; **Fig. 3, Table S2**) i.e., 15 days after the Chl *a* peak, while in 2016 it occurred on 20 June (35.2 mg L^{-1}) i.e., 7 days after the second Chl *a* peak. Fatty acid profiles of sea ice samples were dominated in both 2015 and 2016 by $C_{16:1\Delta7}$ (palmitoleic; 68.9 and 53.6% respectively) and $C_{16:0}$ (palmitic; 26.1 and 30.8% respectively) acids; they also exhibited smaller proportions of $C_{14:0}$ (4.7 and 4.2% respectively), $C_{18:1\Delta9}$ (oleic; 5.4 and 0.3% respectively), EPA (0.4 and 10.3% respectively) and DHA acids (0.0 and 1.2% respectively; **Table 1**). Among the TFA, the contribution of SFA ($C_{14:0}$ and $C_{16:0}$) was relatively similar in 2015 and 2016 (mean ± SE = 30.7 ± 1.9 % and 35.0 ± 2.8 %, respectively). Contributions of MUFA (palmitoleic and oleic acids) were higher in 2015 than in 2016 (mean ± SE = 68.9 ± 2.0 % and 53.6 ± 3.2 %, respectively), while the PUFA (n-3 PUFA EPA and DHA) contribution was lower in 2015 than 2016 (mean ± SE = 0.4 ± 0.3 % and 11.4 ± 1.9 %, respectively; **Table 1**). Absolute concentrations of the different lipid classes were significantly different between the years (Wilcoxon test; *p-value* < 10^{-4}). Although the 2016 Spring was less productive than 2015 Spring in terms of TFA, MUFA and SFA, the PUFA content was higher (mean ± SE = 0.9 ± 0.2 % and 0.2 ± 0.1 mg L^{-1}, respectively; **Table 1**). To unravel how sea ice sampling dates (variables) could be described by their environment (Chl *a*, snow thickness (snow), PAR, air temperature (Temperature), TFA and PUFA), a biplot PCA was performed (**Fig. 4**). The PCA accounted for 64.1% of the total variation among sea ice sampling dates (Axis 1: 44.2% and Axis 2: 19.9%). The sea ice stations (variables) are displayed according to their contribution (in %) to the dimensions of the biplot. The quality of the contribution is colored. In **Fig. 4**, contributions higher than 15 are considered as good (orange, indicator length of arrows). The analysis revealed that TFA, PAR, snow and Chl *a*

are key environmental factors for describing the sea-ice sampling dates, while air temperature and PUFA are of less importance. Overall, the 2015 sea-ice sampling stations were characterized by high snow thickness, Chl *a* and TFA concentrations associated with low PAR, air temperature and PUFA content. Conversely, the 2016 sea-ice sampling period was characterized by relatively low snow thickness and concentrations of Chl *a* and TFA associated with high PAR, air temperature and PUFA content (**Fig. 4**).

HBIs were detected during both sampling years. Because of the slightly different analytical methodology employed for the analysis of HBIs in sea-ice and bivalves, no comparison of absolute HBIs values can be made between the two types of samples. A Wilcoxon test on the different HBIs investigated showed no significant differences between 2015 and 2016 ($p\text{-value} > 0.05$). During both years, IP_{25} and HBI IIa were well correlated in sea ice (Spearman's r = 0.92, $p\text{-value} < 0.01$, n = 51) as well as HBI IIa, III and IV (Spearman's r ranged from 0.87 to 0.94, $p\text{-value} < 0.01$, n = 51) (**Table 2**). Conversely, IP_{25} and HBI IIa were not well correlated with HBI IIb, III or IV (**Table 2**).

3.2 Bivalves

We monitored HBIs in *M. truncata* and *S. groenlandicus* from winter to summer 2015 and 2016 (**Fig. 6**). With the exception of the four last 2015 and two last 2016 sampling dates, *M. truncata* presented higher IP_{25} contents than *S. groenlandicus* (**Fig. 5A, B**). However, the mean IP_{25} content of *S. groenlandicus* was higher than that of *M. truncata* in both 2015 (mean ± SE = 127.9 ± 63.9 and 57.0 ± 15.9 ng g^{-1} dry mass, respectively) and 2016 (mean ± SE = 86.5 ± 52.0 and 37.3 ± 8.0 ng g^{-1} dry mass, respectively). The IP_{25} contents of *S. groenlandicus* collected in 2015 and 2016 presented similar seasonal trends, i.e., an exponential-like curve with low values observed from January to early May, followed by increasing values from May to late June (**Fig. 5A, B**). These increases in *S. groenlandicus*

285 IP_{25} content corresponded to the sea ice production period of IP_{25}. IP_{25} content in *M. truncata*
286 followed the same trend as *S. groenlandicus* during both years, although the trend was not as
287 clear (**Fig. 5A, B**). Similarly to IP_{25}, *S. groenlandicus* HBI III content was higher than in *M.*
288 *truncata* in both 2015 (mean ± SE = 19.3 ± 4.4 and 5.3 ± 0.8 ng g^{-1} dry mass, respectively)
289 and 2016 (mean ± SD = 6.8 ± 3.2 and 3.0 ± 0.5 ng g^{-1} dry mass, respectively). The HBI III
290 contents of *S. groenlandicus* collected in 2015 and 2016 presented similar seasonal trends,
291 i.e., low values observed from January to April/May followed by increasing values from May
292 to late June (**Fig. 5A, B**). In both instances, the increase of *S. groenlandicus* HBI III occurred
293 after HBI III production in sea ice and before IP_{25} accumulation in *S. groenlandicus*. Although
294 the general trend of low HBI III values from January to April/May followed by increasing
295 values from May to late June was also observed for *M. truncata* (at least for 2016; **Fig. 5D**),
296 the increase did not clearly precede that of IP_{25}; nor did it occur after sea-ice HBI production.
297 A strong correlation was observed between IP_{25} and HBI IIa in *S. groenlandicus* over the
298 two years (Spearman's r = 0.99, *p-value* < 0.01, n = 38; **Table 2**). This correlation was also
299 present, but weaker, in sea-ice POM and *M. truncata* (r = 0.92 and 0.44, respectively).
300 Correlations between HBI IIb, III and IV were strong for sea-ice POM, moderate in *S.*
301 *groenlandicus* (r ranged from 0.70 to 0.87) and relatively weak in *M. truncata* (r ranged from
302 0.21 to 0.70).
303 Non-metric multidimensional scaling (nMDS) of bivalve lipid data (i.e., fatty acid and
304 HBI contents) showed that *M. truncata* samples were well grouped, at both seasonal and
305 interannual scales. In contrast, *S. groenlandicus* samples formed a more diffusive group at
306 those same scales (**Fig. 6**). The fatty acid profiles of bivalves were similar to those of sea-ice
307 POM, but occurred in different proportions (**Tables 1, 3, Table S2–S4**). For instance, *S.*
308 *groenlandicus* samples during both 2015 and 2016 were dominated by EPA (mean ± SE =
309 44.9 ± 4.1 and 35.3 ± 5.9% respectively), $C_{16:0}$ (mean ± SE = 20.7 ± 1.0% and 25.6 ± 2.7%

310 respectively) and $C_{16:1\Delta7}$ acids (mean ± SE = 15.8 ± 1.3% and 20.0 ± 2.9% respectively),
311 while exhibiting lower proportions of DHA (mean ± SE = 8.5 ± 0.5% and 6.8 ± 1.0%
312 respectively), $C_{14:0}$ (mean ± SE = 5.7 ± 0.4 and 6.9 ± 0.6% respectively) and $C_{18:1\Delta9}$ acid
313 (mean ± SE = 4.3 ± 0.3% and 5.3 ± 0.8% respectively; **Table 3**). The *M. truncata* samples
314 during both 2015 and 2016 were dominated by EPA (mean ± SE = 42.7 ± 5.9% and 37.4 ±
315 6.0% respectively), $C_{16:0}$ (mean ± SE = 23.8 ± 2.5% and 30.2 ± 3.4% respectively), $C_{16:1\Delta7}$
316 acids (mean ± SE = 12.0 ± 1.7% and 16.5 ± 3.0% respectively) and DHA (mean ± SE = 16.2
317 ± 1.4% and 9.3 ± 0.8% respectively). They also exhibited smaller proportions of $C_{18:1\Delta9}$ (mean
318 ± SE = 4.3 and 3.8 ± 0.7% respectively) and $C_{14:0}$ acids (mean ± SE = 1.9 ± 0.3% and 2.7 ±
319 0.5% respectively; **Table 3).** TFA contents were higher in *S. groenlandicus* than in *M.*
320 *truncata* during both 2015 (mean ± SE = 233.5 ± 19.7 and 40.1 ± 5.0 mg g^{-1} dry mass,
321 respectively) and 2016 (mean ± SE = 167.6 ± 25.2 and 54.6 ± 5.0 mg g^{-1} dry mass,
322 respectively). Among the TFA, the contribution of SFA was relatively similar for the two
323 species during 2015 (mean ± SE = 25.7 ± 2.8 % and 26.4 ± 1.4 %, respectively) and 2016
324 (mean ± SE = 32.9 ± 3.8 % and 32.5 ± 3.7 %, respectively), while the contribution of MUFA
325 was slightly lower in *M. truncata* than in *S. groenlandicus* during 2015 (mean ± SE = 15.2 ±
326 2.2 % and 20.1 ± 1.6 %, respectively) and 2016 (mean ± SE = 20.3 ± 3.7 % and 25.3 ± 3.7 %,
327 respectively; **Table 3**). Conversely, the contribution of PUFA was slightly higher in *M.*
328 *truncata* than in *S. groenlandicus* during 2015 (mean ± SE = 58.9 ± 7.2 % and 53.5 ± 4.6 %,
329 respectively) and 2016 (mean ± SE = 46.7 ± 6.8 % and 42.2 ± 6.9 %, respectively).

330 The temporal evolution of palmitoleic/palmitic acid ratios and of the TFA and PUFA
331 contents of bivalves were monitored during both 2015 and 2016 (**Fig. 7; Table S3, S4**).
332 Values were seasonally steady in *M. truncate,* but for TFA in *S. groenlandicus*, declined from
333 a seasonal maximum at the beginning of sampling (**Fig. 7**). The importance of diatoms for
334 bivalve diet was assessed here with the palmitoleic/palmitic acid ratio, which increases with

the contribution of diatoms to animal biomass (Pedersen et al., 1999; Reuss and Poulsen, 2002). During both years, the ratios of *S. groenlandicus* were higher early in the sampling period (0.98 from 18 January to 21 March 2015 and 0.96 from 07 January to 10 May 2016) than afterwards (0.56 from 03 May to 26 June 2015 and 0.58 from 30 May to 19 June 2016). These low ratios corresponded to the period when bivalve consume sympagic algae (**Fig. 7A, B**). The TFA and PUFA contents of *S. groenlandicus* followed similar qualitative trends. TFA contents were highest early in the season (304.8 and 196 mg g^{-1} dry mass in 2015 and 2016, respectively) and lowest afterwards (108.9 and 82.1 mg g^{-1} dry mass in 2015 and 2016). For PUFA, the values declined from 180.5 and 82.7 in early 2015 and 2016, respectively, to 47.1 and 34.7 mg g^{-1} dry subsequently (**Fig. 7C–F**).

4. Discussion

4.1 Sea ice seasonal and inter-annual lipid productivity

A Principal Component Analysis (PCA) biplot of environmental variables was used to reduce the dimensionality of the sea ice samples (**Fig. 4**). This highlighted that in 2015 the snow cover was thicker than in 2016, which resulted in reduced under-ice PAR. In terms of biomarkers, the 2015 sea ice was characterized by higher Chl *a* concentrations and TFA contents than in 2016, associated with lower PUFA (EPA and DHA) contents. The great difference in Chl *a* productivity may derive from the contrasted atmospheric forcings present during the winters preceding each sampling period. Indeed, the winter of 2014–2015 was colder and with less snowfall than the 2015–2016 winter. As a consequence, twice the amount of light was transmitted to the bottom ice prior to sampling, which could in large part explain the average six times larger sympagic production of Chl *a* in 2015 than 2016 (Oziel et al., 2019; **Fig. 3**). Since larger sympagic Chl *a* biomass was observed in 2015 than 2016, it is not surprising to also observe the largest total fatty acid production in 2015 (**Figs. 3, 4; Table 1**).

Interestingly, a mismatch between TFA and Chl *a* peaks was observed over the two years (**Fig. 3**). This result has already been pointed out by Amiraux et al. (2020) during the 2016 melting season in the same area. Those authors attributed this phenomenon to the photoacclimation of sympagic algae to higher light intensities (derived from snow melting) and the consequent reduction of their Chl *a* content per cell, resulting in a mismatch between Chl *a* and fatty acid peaks. Thus, based on the observation of Chl *a* and fatty acid peak mismatches over the two years, we suggest that this particular feature is probably common to sea ice melt.

The fatty acid profiles of the sea-ice POM obtained in southwest Baffin Bay were similar to those previously reported during spring in Svalbard and the Barents Sea (Henderson et al., 1998; Leu et al., 2011; Leu et al., 2010). However, the relative contribution of different lipid classes somewhat differed from the proportions found in the literature. PUFA contributions were notably low here (0.4 and 11.4% in 2015 and 2016 respectively) relative to those measured in Svalbard and the Barents Sea (> 17%). While the threshold percentage at which the relative contribution of a fatty acid is accounted for differ among fatty acid studies (e.g., 1 or 3%; 3% in the present study) and may have contributed to this contrast, the most likely explanation is a regional or annual difference in the relative production of fatty acids. Absolute concentrations of the different fatty acid classes greatly differed between the sampling years with higher TFA, MUFA and SFA concentration in Spring 2015 than 2016 (**Table 1**). Conversely, sympagic algae collected in Spring 2016 presented higher PUFA absolute concentrations than those of 2015 (mean ± SE = 0.9 ± 0.2 and 0.2 ± 0.1 mg L^{-1} in 2016 and 2015 respectively; **Table 1; Fig. 4**). While the total algal biomass that reaches the seafloor is important for the feeding ecology of bivalves, the nutritional value of this biomass is determined by the essential fatty acids EPA and DHA (Hendriks et al., 2003; Lane, 1987). These PUFAs are essential because most bivalve species are unable to synthesize them from

386 shorter chain precursors (Chu and Greaves, 1991; Delaunay et al., 1993). Thus, we suggest
387 that, although sympagic production was higher in 2015 than 2016 (as attested by e.g., Chl *a*
388 and TFA content), the 2016 sea ice was more useful for bivalves (at least for essential fatty
389 acids) than the 2015 production.

390 In a previous investigation, Amiraux et al. (2019) conducted the first analysis of the
391 temporal evolution of IP_{25} and other HBIs during the 2016 melting season in the same area. In
392 the present study, sea ice HBI analysis was performed on both 2015 and 2016 samples with a
393 different methodology and filters to those reported by Amiraux et al. (2019) in their studies.
394 Belt et al. (2014) warned the 'HBI scientific community' that the absolute quantification of
395 HBIs obtained from different laboratories and/or using different methodologies (e.g.,
396 standard: 9-OHD or 7-HND) may be relatively different. Thus, in order to prevent this bias,
397 the present study only discusses the absolute values obtained by the same method, or else the
398 relative values obtained from different methods (e.g., biomarker correlations).

399 Overall, we confirmed the general findings of Amiraux et al. (2019) for sea-ice POM;
400 namely, the co-occurrences of: (i) IP_{25} and HBI IIa, which is consistent with a single source
401 (sympagic) for the two compounds (Brown et al., 2014a; Brown et al., 2014b; Limoges et al.,
402 2018), and (ii) HBIs IIb, III and IV (**Table 2**). The latter was most likely attributed to a
403 pelagic production at the early sea ice melts stages and within sea ice, by the tube-dwelling
404 diatom *Berkeleya rutilens* (Amiraux et al., 2019). In recent years, numerous HBI-based
405 proxies have been developed (Belt, 2018). Among them, the so-called PIP_{25} index
406 (phytoplankton marker-IP_{25}; Müller et al., 2011) has provided, in some cases, more detailed
407 descriptions of palaeo Arctic sea-ice conditions in sediment records than using IP_{25} alone
408 (e.g., Belt, 2018; Berben et al., 2014; Fahl and Stein, 2012; Müller and Stein, 2014; Müller et
409 al., 2012). On the other hand, the HBI biomarker-based 'H-print' has provided valuable
410 estimates of the relative contributions of sympagic- and pelagic-derived primary production in

411 a variety of Arctic animals (Brown, 2018; Brown et al., 2018; Brown et al., 2014d). The
412 robustness of these proxies depends on whether the markers are unequivocally specific to
413 sympagic and pelagic growth environments, or not. Although IP_{25} appears to represent a
414 suitable sympagic biomarker, due to its source specificity (Brown et al., 2014c), identification
415 of the most suitable pelagic counterpart remains challenging (Belt, 2018). In recent studies,
416 the use of some other HBIs (including HBI III) has been suggested as preferable pelagic
417 counterparts to IP_{25}, owing to their apparently greater source specificity (Belt, 2018; Belt et
418 al., 2018; Belt et al., 2019; Köseoğlu et al., 2018; Smik, 2016). However, data from the
419 current study confirm the findings of Amiraux et al. (2019); namely, that HBI III can occur in
420 sea ice and is not as specific of the pelagic environment as originally believed (**Fig. 5C, D**).
421 HBI production in sea-ice (including IP_{25}) did not significantly differ between years
422 (Wilcoxon test; *p-value* > 0.05). Since IP_{25}-producing species are normally only present as
423 minor components of the ice-algal assemblage (typically 1–5%; Brown et al., 2014c), the
424 combination of a nearly stable IP_{25}-production in years with reduced ice-algal production (as
425 indicated by the Chl *a* or TFA; **Fig. 3**) indicates a relatively high contribution of IP_{25}-
426 producing species in 2016.
427
428 *4.2. Efficiency of benthic-pelagic coupling*
429
430 Pelagic–benthic coupling is known to be particularly tight on Arctic shelves (Ambrose
431 and Renaud, 1997; Clough et al., 2005; Hobson et al., 1995; Renaud et al., 2008; Olivier et
432 al., 2020), with a large portion (48 to 96%) of the carbon produced in the water column falling
433 to the seafloor each year (Wassmann, 1991). Although the relative contribution of sympagic
434 algae and phytoplankton to total marine primary production varies with ice cover and water
435 column productivity, it has been shown that a significant fraction of the carbon reaching the
436 seafloor derives from sympagic algal material (Belt, 2018). The joint monitoring of the sea-

437 ice proxy IP_{25} in both sea ice and the bivalves beneath, allowed us to determine the efficiency
438 of the benthic-pelagic (and more precisely: benthic-sympagic) coupling for two years (**Fig. 5**).
439 Both *M. truncata* and *S. groenlandicus* presented depleted IP_{25} concentrations during winter
440 months, followed by days of rapid enrichment once IP_{25} was produced in sea ice (**Fig. 5 A,**
441 **B**). This pattern confirms that benthos rapidly responded to the influx of sympagic organic
442 matter (days to weeks; Graf, 1989; Renaud et al., 2008). Similarly, bivalves presented
443 depleted HBI III concentrations in winter, followed by a rapid enrichment from ca. April/May
444 (**Fig. 5**). From its presupposed pelagic origin in the marginal ice zone (Belt et al., 2015;
445 Collins et al., 2013; Köseoğlu et al., 2018; Smik, 2016; Smik et al., 2016b), HBI III has only
446 been reported in phytoplankton collected during summer and autumn (Belt et al., 2017). Thus,
447 the enrichment of HBI III in bivalves observed from ca. April/May unlikely derived from
448 open water production. Moreover, in sea ice, the production of HBI III has been reported to
449 occur before that of IP_{25} (**Fig. 5**; Amiraux et al., 2019). Thus, the earlier HBI III enrichment in
450 bivalve flesh compared to IP_{25} strongly supports the notion that these animals ingest sea ice-
451 derived HBI III. Consequently, we suggest that in coastal regions at least, HBI III derived
452 from sea ice reaches the seafloor and contributes to the diet of arctic animals, potentially
453 lowering the robustness of the PIP_{25} and H-print indices.

454 For both years, IP_{25} and HBI III concentrations were more than twice higher in *S.*
455 *groenlandicus* than in *M. truncata.* Moreover, the response of *M. truncata* to sympagic POM,
456 as identified by their HBI enrichment (IP_{25} and HBI III) was less evident than for *S.*
457 *groenlandicus* (**Fig. 5**). An explanation may be found in the size of the organisms collected.
458 Indeed, it has been shown that bivalve filtration rate is to some extent a function of their body
459 size (Riisgård and Møhlenberg, 1979; Riisgård and Seerup, 2003; Sylvester et al., 2005). It
460 follows that the consumption of large-sized sympagic algae by small bivalves should be
461 relatively weak, resulting in a low and more variable HBI enrichment than in large bivalves.

In the present study however, this argument is countered by the heavier mass of *M. truncata* samples compared to *S. groenlandicus* (**Table S1**). A more likely explanation lies in the feeding behaviors of these two bivalves. Indeed, although *S. groenlandicus* and *M. truncata* are both slow-mobile burrowing suspension feeders (Gulliksen and Svensen, 2004; Huber, 2010; McTigue and Dunton, 2014; Shojaei, 2016), their bioturbation affinity differs. Unlike *S. groenlandicus, M. truncata* induces diffusive mixing bioturbation (Lacoste et al., 2018), and is expected to ingest a variable and non-negligible quantity of buried sediment. Although *M. truncata* had higher IP_{25} content than *S. groenlandicus* during winter months (**Fig. 5A, B**), its IP_{25} content was half that of *S. groenlandicus* over the entire season. This result supports the notion that sediment represents a non-negligible part of the diet in *M. truncata*. Indeed, the higher IP_{25} content of *M. truncata* compared to *S. groenlandicus* in winter suggests that sediment POM represents a better source of IP_{25} than primary production during this season. Conversely, the higher spring IP_{25} content in *S. groenlandicus* compared to *M. truncata* suggests that primary production is the better source of IP_{25} during this season. Moreover, since unsaturated lipids (including HBIs) are susceptible to degradative processes in the upper centimeters of the sediment (Rontani and Belt, 2019; Rontani et al., 2018), the consumption of sediment POM by *M. truncata* should provide less and more variable lipid contents (including HBI) than the supposed strict diet of sympagic and pelagic material in *S. groenlandicus*. Lipid contents (**Fig. 5, 7**) and the positive correlations between different HBIs support this interpretation (**Table 2**). Indeed, the correlations between different HBIs in *S. groenlandicus* (i.e., Spearmans'r = 0.99 for IP_{25} and HBI IIa; r ranged from 0.70 to 0.87 for HBI IIb, III and IV; **Table 2**) were as strong as those observed in sea ice, which attests to the almost exclusive contribution of sympagic algae to their diet during the sampling period. By contrast, the relatively weak correlations among HBIs in *M. truncata* (i.e., spearmans'r = 0.44

for IP_{25} and HBI IIa; r ranged from 0.21 to 0.70 for HBI IIb, III and IV) imply a reduced sympagic contribution to their diet.

4.3. Effectiveness of essential fatty acid transfer from sea ice to bivalve

Based on lipid data, nMDS was employed to graphically represent the position of the 75 bivalves by year and species (**Fig. 6**). Unlike for *S. groenlandicus,* data for *M. truncata* samples were well clustered, suggesting low lipid variability among seasons or years. Indeed, *M. truncata* samples were distinguished from those of *S. groenlandicus* by relatively constant and lower fatty acid contents (ca. 6 and 3 times lower in 2015 and 2016 respectively; **Table 3**). This general pattern is reminiscent of that of the HBIs (as previously discussed) and reinforces the interpretation that *M. truncata* relies to a greater extent than *S. groenlandicus* on sedimentary organic matter for feeding.

Although the absolute quantities of lipid classes differed between years and bivalve species, their relative contribution was somewhat similar, with a mean PUFA (herein n-3 PUFA EPA and DHA) contribution to TFA above 40%, irrespective of species and sampling year (**Table 3**). This contribution is similar to those observed in other Arctic bivalves such as *Astarte elliptica* or *Bathyarca glacialis* (Gaillard et al., 2017; Gaillard et al., 2015) and underscores the strong accumulation of these essential plant-derived molecules in benthic filter feeders. The benthos is known to respond rapidly to the influx of sympagic organic matter (days to weeks; Graf, 1989; Renaud et al., 2008), principally due to its relatively high content in n-3 PUFAs (Arrigo and Thomas, 2004). We confirmed, through HBI analysis, that sympagic material was quickly assimilated by *M. truncata* and *S. groenlandicus* after 21 April in 2015 and after 10 May in 2016 (**Fig. 5A, B**).

Since we argued previously that sympagic/pelagic-benthic coupling is relatively weak for *M. truncate*, we will hereafter focus on *S. groenlandicus* to assess the impact of sympagic

512 fatty acid deliveries on the quality of bivalve flesh. Diatoms represent the dominant taxon of
513 sympagic algae (Amiraux et al., 2019; Brown et al., 2016; Ratkova and Wassmann, 2005) and
514 are known as good producers of EPA (Kelly and Scheibling, 2012; Viso and Marty, 1993),
515 which was the main n-3 PUFA present in our bivalve samples (**Table 3**). It is therefore not
516 surprising that the palmitoleic/palmitic acid ratio, as well as the TFA and PUFA contents,
517 were similar during both sampling years (**Fig. 7**). *S. groenlandicus* harvested before the
518 period of peak algal production were then characterized by relatively high
519 palmitoleic/palmitic ratios consistent with relatively strong diatom contribution to their lipid
520 reserves. By contrast, these ratios were low in *S. groenlandicus* specimens feeding on
521 sympagic algae (as attested by HBI measurements), at or near the apogee of the productive
522 period in sea ice (**Table 3; Fig. 7**). While this apparent diminution of the diatom signal is
523 unexpected at a time when ice algal deliveries to the sea floor increase, prior studies have
524 shown that the deposition of sympagic algal biomass onto the seafloor is particularly
525 important early in the spring when the intake of C and n-3 PUFA is required to jumpstart
526 benthic growth and reproduction after the food limited winter (McMahon et al., 2006; North
527 et al., 2014). Thus, these seemingly low sympagic POM intakes by bivalves result most likely
528 from their quick utilization of this organic matter (newly delivered or previously stored),
529 rather than from a low contribution.

530 The reproduction of intertidal bivalves includes gametogenesis, development and
531 metamorphosis, all of which are energy-consuming processes (Martinez et al., 2000). The
532 success of these processes depends on the overall physiological condition and especially the
533 pre-spawning condition of the adults. The larger the build-up of storage material, the more
534 weight loss the animal can incur at spawning without endangering its subsequent survival and
535 growth (Beukema et al., 2001). In the present study, we identified the spawning period from
536 the intake of sympagic material by the bivalves (indicated by IP_{25} enrichment; **Fig. 5**) and the

steep concurrent decrease in their fatty acid content (**Fig. 7**). Although the pre-spawning conditions were different among years and bivalve species (e.g., the initial PUFA dry mass of *S. groenlandicus* was two-fold higher from 18 January to 21 April 2015 and from 07 January to 10 May 2016 respectively), on the last sampling day of both years the two species presented similar n-3 PUFA contents, but differed in their TFA contents (**Table S3, S4**). This pattern suggests that the n-3 PUFA content observed at the end of the sampling period represents the residual amount necessary to ensure organism survival once it has completed its spawning effort. The fact that pre-spawning n-3 PUFA and TFA contents in *M. truncata* were lower than their post-spawning values in 2015 (**Fig. 7**), suggests that the animals were then unable to acquire enough essential fatty acids for the reproductive effort, which may have been delayed or suppressed in that year.

Conclusion

We examined the contents of n-3 PUFA and HBIs of sea ice POM and two different filter-feeding bivalve species during two Arctic melting seasons that took place in southwest Baffin Bay. The results underscored a relatively strong seasonal and interannual variability in the production of organic matter (whether fatty acid or chlorophyll *a*) and biomarkers in sea ice, due to different conditions of air temperature, snow deposition and transmitted PAR. The sea ice nevertheless shared many common characteristics during the two melting seasons, including (i) a similar productivity of IP_{25}, (ii) a production of the so-called HBI pelagic biomarker HBI III that seasonally preceded that of IP_{25}, (iii) a temporal mismatch between chlorophyll *a* and fatty acid production peaks. Although Spring 2015 was the most productive for nearly all the parameters analyzed (e.g., TFA, Chl *a*), Spring 2016 was the most productive in terms of the lipids considered essential (the n-3 PUFAs EPA and DHA) for the growth and reproduction of bivalves. By tracking the different HBIs, their levels and the correlations between each of those, we (i) confirmed that sympagic-benthic coupling is tight

on Arctic shelves (ii) showed that unlike *M. truncata, S. groenlandicus* can be used as a responsive sentinel of pelagic-benthic coupling, and (iii) confirmed that HBI III is present in sea ice, which may weaken the robustness of some HBI-based proxies. By monitoring the fatty acid content of bivalves from winter to late spring, we (i) showed that these animals greatly accumulate essential fatty acids (mean relative contributions exceeding 40%), (ii) identified their pre-spawning and post-spawning periods, and (iii) proposed that *M. truncata* may fail to store enough essential fatty acids to support its reproductive effort in some years.

Acknowledgements

We especially thank E. Brossier for the sampling of bivalves, C. Guilmette and F. Dufour for providing preliminary lipid results. This project was made possible by the support of the hamlet of Qikiqtarjuaq and the members of the community together with the Inuksuit School and its Principal, Jacqueline Arsenault. It was conducted under the scientific coordination of the Canada Excellence Research Chair on Remote Sensing of Canada's new Arctic frontier and the CNRS & Université Laval Takuvik Joint International Laboratory (UMI3376). The field campaigns (Scientific Research License # 01 010 15N-M and # 01 001 16R-M) owed its success to the contribution of J. Ferland, G. Bécu, C. Marec, J. Lagunas, F. Bruyant, J. Larivière, E. Rehm, S. Lambert-Girard, C. Aubry, C. Lalande, A. LeBaron, C. Marty, J. Sansoulet, D. Christiansen-Stowe, A. Wells, M. Benoît-Gagné, E. Devred and M.-H. Forget from the Takuvik Laboratory, C.J. Mundy from the University of Manitoba and F. Pinczon du Sel and E. Brossier from Vagabond. We also thank the FRQNT strategic network Québec-Océan, the CCGS *Amundsen* and the Polar Continental Shelf Program for their in-kind contribution in polar logistics and scientific equipment. We especially thank C. Nozais from the Université du Québec à Rimouski for providing the sediment traps, C. Lalande (Project leader), C. Aubry, and T. Dezutter from the Université Laval Joint International Laboratory and Takuvik Laboratory for allowing the 2016 short-term sediment trap deployment. This

589 work contributes to the scientific programs of Takuvik and Québec-Océan. We are grateful to
590 the two anonymous reviewers, for providing helpful comments on a previous version of the
591 manuscript.

592

593

594

595 **Funding information**

596

597 The first author (RA) received financial support from the Université Bretagne Loire
598 (UBL) "post-doctoral attractiveness" program and the Sentinel North postdoctoral program of
599 Université Laval, made possible in part by funding from the Canada First Research
600 Excellence Fund. RA also received a postdoctoral grant from the Littoral Research Chair at
601 Université Laval, which is mainly funded by Sentinel North and the Northern Contaminant
602 Program of the Crown and Indigenous Relations and Northern Affairs Canada. This research
603 was supported by the GreenEdge project, which was funded by the following French and
604 Canadian programs and agencies: ANR (Contract #111112), CNES (project #131425), IPEV
605 (project #1164), CSA, Foundation Total, ArcticNet, LEFE and the French Arctic Initiative
606 (Green Edge project).

607 **Competing interests**

608 The authors declare that they have no competing interests.

609

610 **Supplemental material**

611 There are four pieces of supplemental material (Table S1, S2, S3, S4).

612

613 **Data accessibility statement**

614 All data are accessible at the Green Edge database (http://www.obs-
615 vlfr.fr/proof/php/GREENEDGE/greenedge.php) and will be made public after publication.

616

Figure caption

Figure 1: Numbering system used to describe structural characteristics of highly branched isoprenoids (I) and structures of some common C_{25} highly branched isoprenoids (IP_{25} – IV).

Figure 2: Map of the study area with location of the station investigated in southwest Baffin Bay.

Figure 3: Time series of chlorophyll *a* and total fatty acid concentration in the bottom 0–3 cm sea ice section from (**A**) 25 April to 24 June 2015 and from (**B**) 16 May to 8 July 2016 at the sampling location in southwest Baffin Bay (**Fig. 2**).

Figure 4: Principal Component analysis (PCA) biplot representing the distribution of sea ice samples collected at different sampling time and year according to the environmental core variables: chlorophyll a (Chl a), snow thickness (Snow), air temperature (Temperature), photosynthetically active radiation (PAR). total fatty acid (TFA) and polyunsaturated fatty acid content (PUFA). The PCA accounts for 64.1% of the total variation among sea ice sampling dates (Axis 1: 44.2% and Axis 2: 19.9%). The environmental variables are displayed according to their contribution (%) to the dimensions of the biplot. The quality of the contribution is colored (good contribution should be higher than 15: orange, indicator length of arrow).

Figure 5: Time series of IP_{25} (**A, B**) and HBI III (**C, D**) in sea ice (watermark) and bivalve collected from (**A, C**) 25 April to 24 June 2015 and from (**B, D**) 16 May to 8 July 2016 at the sampling location in southwest Baffin Bay (**Fig. 2**).

Figure 6: Non-metric multidimensional scaling (nMDS), based on the Euclidean distance on normalized lipid data (HBI and fatty acids) representing the position of the 75 bivalves collected species (*Mya truncata* or *Serripes groenlandicus*) and sampling year (2015 or 2016) on the ordination diagram. 2D stress = 0.06.

Figure 7: Time series of palmitoleic/palmitic acid ratio (**A, B),** total fatty acid (**C, D**) and polyunsaturated fatty acid content (**E, F**) in *Mya truncata* and *Serripes groenlandicus* collected from (**A, C, E**) 25 April to 24 June 2015 and from (**B, D, F**) 16 May to 8 July 2016 at the sampling location in southwest Baffin Bay (**Fig. 2**).

Table 1: Mean fatty acid composition, expressed as mass % of total fatty acids (TFA), of POM collected in the 0–3 cm of sea ice in Davis strait between 24 April to 24 June 2015 and, 16 May to 8 July 2016. Fatty acids above > 3% in at least one of the sea ice sampling investigated were included. TFA = total fatty acids expressed in mg L^{-1}; SFA = saturated fatty acid; MUFA = monounsaturated fatty acid; PUFA = polyunsaturated fatty acid. Values are means (SE).

Table 2: Correlation coefficients between chlorophyll *a* (Chl *a*) and HBI biomarkers in sea ice POM, *Serripes groenlandicus* and *Mya truncata* collected in 2015 and 2016 in southwest Baffin Bay (**Fig. 2**).

Table 3: Mean fatty acid composition, expressed as mass % of total fatty acids (TFA), of (A) *Serripes groenlandicus* and (B) *Mya truncata* collected in Davis strait between January and June 2015 and between January and June 2016. Fatty acids above >3% in at least one of the bivalve sampling investigated were included. TFA = total fatty acids expressed in mg g^{-1} dry mass; SFA = saturated fatty acid; MUFA = monounsaturated fatty acid; PUFA = polyunsaturated fatty acid. Values are mean (SE).

References

Ambrose, W.G., Renaud, P.E., 1997. Does a pulsed food supply to the benthos affect polychaete recruitment patterns in the Northeast Water Polynya? Journal of Marine Systems 10, 483-495.

Amiraux, R., Belt, S.T., Vaultier, F., Galindo, V., Gosselin, M., Bonin, P., Rontani, J.-F., 2017. Monitoring photo-oxidative and salinity-induced bacterial stress in the Canadian Arctic using specific lipid tracers. Marine Chemistry 194, 89-99.

Amiraux, R., Burot, C., Bonin, P., Guasco, S., Babin, M., Rontani, J.-F., 2020. Stress factors resulting from the Arctic vernal sea ice melt: impact on the viability of the bacterial communities associated to sympagic algae. Elementa: Science of the Anthropocene (in press).

Amiraux, R., Smik, L., Köseoğlu, D., Rontani, J.-F., Galindo, V., Grondin, P.-L., Babin, M., Belt, S.T., 2019. Temporal evolution of IP_{25} and other highly branched isoprenoid lipids in sea ice and the underlying water column during an Arctic melting season. Elementa: Science of the Anthropocene 7. DOI: https://doi.org/10.1525/elementa.377.

Arrigo, K.R., Thomas, D.N., 2004. Large scale importance of sea ice biology in the Southern Ocean. Antarctic Science 16, 471-486.

Bates, S.S., Cota, G.F., 1986. Fluorescence induction and photosynthetic responses of Arctic ice algae to sample treatement and salinity. Journal of phycology 22, 421-429.

Belt, S.T., 2018. Source-specific biomarkers as proxies for Arctic and Antarctic sea ice. Organic Geochemistry 125, 277-298.

Belt, S.T., Allard, W.G., Massé, G., Robert, J.-M., Rowland, S.J., 2000. Highly branched isoprenoids (HBIs): identification of the most common and abundant sedimentary isomers. Geochimica et Cosmochimica Acta 64, 3839-3851.

Belt, S.T., Brown, T.A., Ampel, L., Cabedo-Sanz, P., Fahl, K., Kocis, J., Massé, G., Navarro-Rodriguez, A., Ruan, J., Xu, Y., 2014. An inter-laboratory investigation of the Arctic sea ice biomarker proxy IP_{25} in marine sediments: key outcomes and recommendations. Climate of the Past 10, 155-166.

Belt, S.T., Brown, T.A., Navarro-Rodriguez, A., Cabedo-Sanz, P., Tonkin, A., Ingle, R., 2012. A reproducible method for the extraction, identification and quantification of the Arctic sea ice proxy IP_{25} from marine sediments. Analytical Methods 4, 705-713.

Belt, S.T., Brown, T.A., Smik, L., Assmy, P., Mundy, C., 2018. Sterol identification in floating Arctic sea ice algal aggregates and the Antarctic sea ice diatom *Berkeleya adeliensis*. Organic geochemistry 118, 1-3.

Belt, S.T., Brown, T.A., Smik, L., Tatarek, A., Wiktor, J., Stowasser, G., Assmy, P., Allen, C.S., Husum, K., 2017. Identification of C25 highly branched isoprenoid (HBI) alkenes in diatoms of the genus *Rhizosolenia* in polar and sub-polar marine phytoplankton. Organic Geochemistry 110, 65-72.

Belt, S.T., Cabedo-Sanz, P., Smik, L., Navarro-Rodriguez, A., Berben, S.M.P., Knies, J., Husum, K., 2015. Identification of paleo Arctic winter sea ice limits and the marginal ice zone: Optimised biomarker-based reconstructions of late Quaternary Arctic sea ice. Earth and Planetary Science Letters 431, 127-139.

Belt, S.T., Massé, G., Rowland, S.J., Poulin, M., Michel, C., LeBlanc, B., 2007. A novel chemical fossil of palaeo sea ice: IP_{25}. Organic Geochemistry 38, 16-27.

Belt, S.T., Smik, L., Brown, T.A., Kim, J.H., Rowland, S.J., Allen, C.S., Gal, J.K., Shin, K.H., Lee, J.I., Taylor, K.W.R., 2016. Source identification and distribution reveals the potential of the geochemical Antarctic sea ice proxy IPSO25. Nature Communications 7.DOI: https://doi.org/10.1038/ncomms12655.

Belt, S.T., Smik, L., Köseoğlu, D., Knies, J., Husum, K., 2019. A novel biomarker-based proxy for the spring phytoplankton bloom in Arctic and sub-arctic settings–HBI T25. Earth and Planetary Science Letters 523, 115703.

Berben, S., Husum, K., Cabedo-Sanz, P., Belt, S., 2014. Holocene sub-centennial evolution of Atlantic water inflow and sea ice distribution in the western Barents Sea. Climate of the Past 10, 181-198.

Beukema, J., Drent, J., Honkoop, P., 2001. Maximizing lifetime egg production in a Wadden Sea population of the tellinid bivalve *Macoma balthica*: a trade-off between immediate and future reproductive outputs. Marine Ecology Progress Series 209, 119-129.

Boetius, A., Albrecht, S., Bakker, K., Bienhold, C., Felden, J., Fernández-Méndez, M., Hendricks, S., Katlein, C., Lalande, C., Krumpen, T., Nicolaus, M., Peeken, I., Rabe, B., Rogacheva, A., Rybakova, E., Somavilla, R., Wenzhöfer, F., Party, R.P.A.-.-S.S., 2013. Export of Algal Biomass from the Melting Arctic Sea Ice. Science 339, 1430-1432.

Brown, T., Alexander, C., Yurkowski, D., Ferguson, S., Belt, S., 2014a. Identifying variable sea ice carbon contributions to the Arctic ecosystem: A case study using highly branched isoprenoid lipid biomarkers in Cumberland Sound ringed seals. Limnology and oceanography 59, 1581-1589.

Brown, T.A., 2018. Stability of the lipid biomarker H-Print within preserved animals. Polar Biology 41, 1901-1905.

Brown, T.A., Assmy, P., Hop, H., Wold, A., Belt, S.T., 2017. Transfer of ice algae carbon to ice-associated amphipods in the high-Arctic pack ice environment. Journal of Plankton Research 39, 664-674.

Brown, T.A., Belt, S.T., 2012. Identification of the sea ice diatom biomarker IP_{25} in Arctic benthic macrofauna: direct evidence for a sea ice diatom diet in Arctic heterotrophs. Polar Biology 35, 131-137.

Brown, T.A., Belt, S.T., Cabedo-Sanz, P., 2014b. Identification of a novel di-unsaturated C25 highly branched isoprenoid in the marine tube-dwelling diatom *Berkeleya rutilans*. Environmental Chemistry Letters 12, 455-460.

Brown, T.A., Belt, S.T., Gosselin, M., Levasseur, M., Poulin, M., Mundy, C.J., 2016. Quantitative estimates of sinking sea ice particulate organic carbon based on the biomarker IP_{25}. Marine Ecology Progress Series 546, 17-29.

Brown, T.A., Belt, S.T., Tatarek, A., Mundy, C.J., 2014c. Source identification of the Arctic sea ice proxy IP_{25}. Nature Communications 5. DOI: https://doi.org/10.1038/ncomms5197.

Brown, T.A., Galicia, M.P., Thiemann, G.W., Belt, S.T., Yurkowski, D.J., Dyck, M.G., 2018. High contributions of sea ice derived carbon in polar bear (*Ursus maritimus*) tissue. PloS one 13, e0191631.

Brown, T.A., Yurkowski, D.J., Ferguson, S.H., Alexander, C., Belt, S.T., 2014d. H-Print: a new chemical fingerprinting approach for distinguishing primary production sources in Arctic ecosystems. Environmental Chemistry Letters 12, 387-392.

Chu, F.-L., Greaves, J., 1991. Metabolism of palmitic, linoleic, and linolenic acids in adult oysters, Crassostrea virginica. Marine Biology 110, 229-236.

Clough, L.M., Renaud, P.E., Ambrose Jr, W.G., 2005. Impacts of water depth, sediment pigment concentration, and benthic macrofaunal biomass on sediment oxygen demand in the western Arctic Ocean. Canadian Journal of Fisheries and Aquatic Sciences 62, 1756-1765.

Collins, L.G., Allen, C.S., Pike, J., Hodgson, D.A., Weckström, K., Massé, G., 2013. Evaluating highly branched isoprenoid (HBI) biomarkers as a novel Antarctic sea-ice proxy in deep ocean glacial age sediments. Quaternary Science Reviews 79, 87-98.

Delaunay, F., Marty, Y., Moal, J., Samain, J.-F., 1993. The effect of monospecific algal diets on growth and fatty acid composition of *Pecten maximus* (L.) larvae. Journal of Experimental Marine Biology and Ecology 173, 163-179.

Dupont, F., 2012. Impact of sea-ice biology on overall primary production in a biophysical model of the pan-Arctic Ocean. Journal of Geophysical Research: Oceans 117. DOI: https://doi.org/10.1029/2011JC006983.

Fahl, K., Stein, R., 2012. Modern seasonal variability and deglacial/Holocene change of central Arctic Ocean sea-ice cover: New insights from biomarker proxy records. Earth and Planetary Science Letters 351-352, 123-133.

Falk-Petersen, S., Sargent, J.R., Henderson, J., Hegseth, E.N., Hop, H., Okolodkov, Y.B., 1998. Lipids and fatty acids in ice algae and phytoplankton from the Marginal Ice Zone in the Barents Sea. Polar Biology 20, 41-47.

Fernández-Méndez, M., Katlein, C., Rabe, B., Nicolaus, M., Peeken, I., Bakker, K., Flores, H., Boetius, A., 2015. Photosynthetic production in the central Arctic Ocean during the record sea-ice minimum in 2012. Biogeosciences 12, 3525-3549.

Gaillard, B., Meziane, T., Tremblay, R., Archambault, P., Blicher, M.E., Chauvaud, L., Rysgaard, S., Olivier, F., 2017. Food resources of the bivalve *Astarte elliptica* in a sub-Arctic fjord: a multi-biomarker approach. Marine Ecology Progress Series 567, 139-156.

Gaillard, B., Meziane, T., Tremblay, R., Archambault, P., Layton, K.K., Martel, A.L., Olivier, F., 2015. Dietary tracers in *Bathyarca glacialis* from contrasting trophic regions in the Canadian Arctic. Marine Ecology Progress Series 536, 175-186.

Garrison, D.L., Buck, K.R., 1986. Organism losses during ice melting: A serious bias in sea ice community studies. Polar Biology 6, 237-239.

Gosselin, M., Legendre, L., Therriault, J.C., Demers, S., Rochet, M., 1986. Physical control of the horizontal patchiness of sea ice microalgae. Marine Ecology Progress Series 29, 289-298.

Gosselin, M., Levasseur, M., Wheeler, P.A., Horner, R.A., Booth, B.C., 1997. New measurements of phytoplankton and ice algal production in the Arctic Ocean. Deep Sea Research Part II 44, 1623-1644.

Graf, G., 1989. Benthic-pelagic coupling in a deep-sea benthic community. Nature 341, 437.

Gulliksen, B., Svensen, E., 2004. Svalbard and life in polar oceans. Kom forlag, Kristiansund, Norway. ISBN: 8292496033.

Harning, D.J., Jennings, A.E., Köseoğlu, D., Belt, S.T., Geirsdóttir, Á., Sepúlveda, J., 2020. Response of biological productivity to North Atlantic marine front migration during the Holocene. Climate of the Past Discussions, 1-26.

Henderson, R., Hegseth, E., Park, M., 1998. Seasonal variation in lipid and fatty acid composition of ice algae from the Barents Sea. Polar Biology 20, 48-55.

Hendriks, I.E., van Duren, L.A., Herman, P.M., 2003. Effect of dietary polyunsaturated fatty acids on reproductive output and larval growth of bivalves. Journal of Experimental Marine Biology and Ecology 296, 199-213.

Hobson, K.A., Ambrose Jr, W.G., Renaud, P.E., 1995. Sources of primary production, benthic-pelagic coupling, and trophic relationships within the Northeast Water Polynya: insights from $d^{13}C$ and $d^{15}N$ analysis. Marine Ecology Progress Series 128, 1-10.

Horner, R., Schrader, G., 1982. Relative contributions of ice algae, phytoplankton, and benthic microalgae to primary production in nearshore regions of the Beaufort Sea. Arctic, 485-503.

Huber, M., 2010. Compendium of Bivalves. ConchBooks, Hackenheim.

Katlein, C., Arndt, S., Nicolaus, M., Perovich, D.K., Jakuba, M.V., Suman, S., Elliott, S., Whitcomb, L.L., McFarland, C.J., Gerdes, R., 2015. Influence of ice thickness and surface properties on light transmission through A rctic sea ice. Journal of Geophysical Research: Oceans 120, 5932-5944.

Kelly, J.R., Scheibling, R.E., 2012. Fatty acids as dietary tracers in benthic food webs. Marine Ecology Progress Series, 446, 1-22.

Köseoğlu, D., Belt, S.T., Smik, L., Yao, H., Panieri, G., Knies, J., 2018. Complementary biomarker-based methods for characterising Arctic sea ice conditions: A case study comparison between multivariate analysis and the PIP_{25} index. Geochimica et Cosmochimica Acta 222, 406-420.

Lacoste, É., Piot, A., Archambault, P., McKindsey, C.W., Nozais, C., 2018. Bioturbation activity of three macrofaunal species and the presence of meiofauna affect the abundance and composition of benthic bacterial communities. Marine Environmental Research 136, 62-70.

Lane, A.J., 1987. The effect of a microencapsulated fatty acid diet on larval production in the European flat oyster *Ostrea edulis* L. University of Wales (UCNW, Bangor: Ocean Sciences).

Leonardos, N., Lucas, I.A., 2000. The nutritional value of algae grown under different culture conditions for *Mytilus edulis* L. larvae. Aquaculture 182, 301-315.

Leu, E., Søreide, J.E., Hessen, D.O., Falk-Petersen, S., Berge, J., 2011. Consequences of changing sea-ice cover for primary and secondary producers in the European Arctic shelf seas: Timing, quantity, and quality. Progress in Oceanography 90, 18-32.

Leu, E., Wiktor, J., søreide, J.E., Berge, J., Falk-Petersen, S., 2010. Increased irradiance reduces food quality of sea ice algae. Marine Ecology Progress Series 411, 49-60.

Limoges, A., Massé, G., Weckström, K., Poulin, M., Ellegaard, M., Heikkilä, M., Geilfus, N.-X., Sejr, M.K., Rysgaard, S., Ribeiro, S., 2018. Spring Succession and Vertical Export of Diatoms and IP_{25} in a Seasonally Ice-Covered High Arctic Fjord. Frontiers in Earth Science 6, 226.

Lovvorn, J.R., Cooper, L.W., Brooks, M.L., De Ruyck, C.C., Bump, J.K., Grebmeier, J.M., 2005. Organic matter pathways to zooplankton and benthos under pack ice in late winter and open water in late summer in the north-central Bering Sea. Marine Ecology Progress Series 291, 135-150.

Martinez, G., Brokordt, K., Aguilera, C., Soto, V., Guderley, H., 2000. Effect of diet and temperature upon muscle metabolic capacities and biochemical composition of gonad and muscle in *Argopecten purpuratu*s Lamarck 1819. Journal of Experimental Marine Biology and Ecology 247, 29-49.

Massé, G., Belt, S.T., Crosta, X., Schmidt, S., Snape, I., Thomas, D.N., Rowland, S.J., 2011. Highly branched isoprenoids as proxies for variable sea ice conditions in the Southern Ocean. Antarctic Science 23, 487-498.

Massicotte, P., Amiraux, R., Amyot, M.-P., Archambault, P., Ardyna, M., Arnaud, L., Artigue, L., Aubry, C., Ayotte, P., Bécu, G., 2019. Green Edge ice camp campaigns: understanding the processes controlling the under-ice Arctic phytoplankton spring bloom. Earth System Science Data 12, 151–176.

Massicotte, P., Bécu, G., Lambert-Girard, S., Leymarie, E., Babin, M., 2018. Estimating underwater light regime under spatially heterogeneous sea ice in the Arctic. Applied Sciences 8, 2693.

McMahon, K.W., Ambrose Jr, W.G., Johnson, B.J., Yi Sun, M., Lopez, G.R., Clough, L.M., Carroll, M.L., 2006. Benthic community response to ice algae and phytoplankton in Ny Ålesund, Svalbard. Marine Ecology Progress Series 310, 1-14.

McTigue, N.D., Dunton, K.H., 2014. Trophodynamics and organic matter assimilation pathways in the northeast Chukchi Sea, Alaska. Deep Sea Research Part II: Topical Studies in Oceanography 102, 84-96.

Morata, N., Renaud, P.E., 2008. Sedimentary pigments in the western Barents Sea: A reflection of pelagic-benthic coupling? Deep Sea Research Part II: Topical Studies in Oceanography 55, 2381-2389.

Müller, J., Stein, R., 2014. High-resolution record of late glacial and deglacial sea ice changes in Fram Strait corroborates ice–ocean interactions during abrupt climate shifts. Earth and Planetary Science Letters 403, 446-455.

Müller, J., Wagner, A., Fahl, K., Stein, R., Prange, M., Lohmann, G., 2011. Towards quantitative sea ice reconstructions in the northern North Atlantic: A combined biomarker and numerical modelling approach. Earth and Planetary Science Letters 306, 137-148.

Müller, J., Werner, K., Stein, R., Fahl, K., Moros, M., Jansen, E., 2012. Holocene cooling culminates in sea ice oscillations in Fram Strait. Quaternary Science Reviews 47, 1-14.

Napolitano, G.E., Ackman, R.G., Ratnayake, W.M., 1990. Fatty acid composition of three cultured algal species (*isochvysis galbana*, *chaetoceros gracilis* and *chaetoceros calcitrans*) used as food for bivalve larvae. Journal of the World Aquaculture Society 21, 122-130.

North, C.A., Lovvorn, J.R., Kolts, J.M., Brooks, M.L., Cooper, L.W., Grebmeier, J.M., 2014. Deposit-feeder diets in the Bering Sea: potential effects of climatic loss of sea ice-related microalgal blooms. Ecological applications 24, 1525-1542.

Olivier, F., Gaillard, B., Thébault, J., Meziane, T., Tremblay, R., Dumont, D., S, B., Gosselin, M., Jolivet, A., Chauvaud, L., Martel, A.L., Rysgaard, S., Olivier, A.-H., Pettré, J., Mars, J., Gerber, S., Archambault, P., 2020. Shells of the bivalve *Astarte moerchi* give new evidence of a strong pelagic-benthic coupling's shift occurring since the late 70s in the NOW Polynya. Philosophical Transactions of the Royal Society A, 378 (2181), 20190353.

Oziel, L., Massicotte, P., Randelhoff, A., Ferland, J., Vladoiu, A., Lacour, L., Lambert-Girard, S., Dumont, D., Cuypers, Y., Bouruet-Aubertot, P., Galindo, V., Marec, C., Forget, M.-H., Garcia, N., Raimbault, P., Houssais, M.-N., Babin, M., 2019. Environmental factors influencing the seasonal dynamics of under-ice spring blooms in Baffin Bay. Elementa: Science of the Anthropocene, 7(1), 34.

Pabi, S., van Dijken, G.L., Arrigo, K.R., 2008. Primary production in the Arctic Ocean, 1998–2006. Journal of Geophysical Research: Oceans 113. DOI: https://doi.org/10.1029/2007JC004578.

Pagès, J., 2004. Analyse factorielle de donnees mixtes: principe et exemple d'application. Revue de Statistique Appliquée LII, 93–111.

Parsons, T., Maita, Y., Lalli, C., 1984. A manual of chemical and biological methods for seawater analysis. Pergamon Press, Totronto. ISBN: 0080302874.

Pedersen, L., Jensen, H.M., Burmeister, A., Hansen, B.W., 1999. The significance of food web structure for the condition and tracer lipid content of juvenile snail fish (Pisces: *Liparis spp.*) along 65-72°N off West Greenland. Journal of Plankton Research 21, 1593-1611.

Poulin, M., Daugbjerg, N., Gradinger, R., Ilyash, L., Ratkova, T., von Quillfeldt, C., 2011. The pan-Arctic biodiversity of marine pelagic and sea-ice unicellular eukaryotes: a first-attempt assessment. Marine Biodiversity 41, 13-28.

Ratkova, T.N., Wassmann, P., 2005. Sea ice algae in the White and Barents seas: composition and origin. Polar Research 24, 95-110.

Renaud, P.E., Morata, N., Carroll, M.L., Denisenko, S.G., Reigstad, M., 2008. Pelagic-benthic coupling in the western Barents Sea: Processes and time scales. Deep Sea Research Part II: Topical Studies in Oceanography 55, 2372-2380.

Reuss, N., Poulsen, L., 2002. Evaluation of fatty acids as biomarkers for a natural plankton community. A field study of a spring bloom and a post-bloom period off West Greenland. Marine Biology 141, 423-434.

Riebesell, U., Schloss, I., Smetacek, V., 1991. Aggregation of algae released from melting sea ice - Implications for seeding and sedimentation. Polar Biology 11, 239-248.

Riisgård, H.U., Møhlenberg, F., 1979. An improved automatic recording apparatus for determining the filtration rate of *Mytilus edulis* as a function of size and algal concentration. Marine Biology 52, 61-67.

Riisgård, H.U., Seerup, D.F., 2003. Filtration rates in the soft clam *Mya arenaria*: effects of temperature and body size. Sarsia 88, 416-428.

Rontani, J.-F., Belt, S.T., 2019. Photo-and autoxidation of unsaturated algal lipids in the marine environment: an overview of processes, their potential tracers, and limitations. Organic Geochemistry 139, 103941.

Rontani, J.-F., Belt, S.T., Amiraux, R., 2018. Biotic and abiotic degradation of the sea ice diatom biomarker IP_{25} and selected algal sterols in near-surface Arctic sediments. Organic Geochemistry 118, 73-88.

Roy, V., Iken, K., Gosselin, M., Tremblay, J.-É., Bélanger, S., Archambault, P., 2015. Benthic faunal assimilation pathways and depth-related changes in food-web structure across the Canadian Arctic. Deep Sea Research Part I: Oceanographic Research Papers 102, 55-71.

Shojaei, M., 2016. Developments in German Bight benthic ecology driven by climate change and anthropogenic utilisation. Doctoral dissertation, University Bremen, Germany.

Smik, L., 2016. Development of biomarker-based proxies for paleo sea-ice reconstructions. Doctoral dissertation, University of Plymouth, United Kingdom.

Smik, L., Belt, S.T., Lieser, J.L., Armand, L.K., Leventer, A., 2016a. Distributions of highly branched isoprenoid alkenes and other algal lipids in surface waters from East Antarctica:

939 Further insights for biomarker-based paleo sea-ice reconstruction. Organic Geochemistry 95,
940 71-80.

941 Smik, L., Cabedo-Sanz, P., Belt, S.T., 2016b. Semi-quantitative estimates of paleo Arctic sea
942 ice concentration based on source-specific highly branched isoprenoid alkenes: A further
943 development of the PIP_{25} index. Organic Geochemistry 92, 63-69.

944 Smith, S.D., Muench, R.D., Pease, C.H., 1990. Polynyas and leads: An overview of physical
945 processes and environment. Journal of Geophysical Research: Oceans 95, 9461-9479.

946 Søreide, J.E., Falk-Petersen, S., Hegseth, E.N., Hop, H., Carroll, M.L., Hobson, K.A.,
947 Blachowiak-Samolyk, K., 2008. Seasonal feeding strategies of Calanus in the high-Arctic
948 Svalbard region. Deep Sea Research Part II: Topical Studies in Oceanography 55, 2225-2244.

949 Sun, M.-Y., Clough, L.M., Carroll, M.L., Dai, J., Ambrose Jr, W.G., Lopez, G.R., 2009.
950 Different responses of two common Arctic macrobenthic species (*Macoma balthica* and
951 *Monoporeia affinis*) to phytoplankton and ice algae: Will climate change impacts be species
952 specific? Journal of Experimental Marine Biology and Ecology 376, 110-121.

953 Sylvester, F., Dorado, J., Boltovskoy, D., Juárez, Á., Cataldo, D., 2005. Filtration rates of the
954 invasive pest bivalve Limnoperna fortunei as a function of size and temperature.
955 Hydrobiologia 534, 71-80.

956 Tesi, T., Belt, S., Gariboldi, K., Muschitiello, F., Smik, L., Finocchiaro, F., Giglio, F.,
957 Colizza, E., Gazzurra, G., Giordano, P., 2020. Resolving sea ice dynamics in the north-
958 western Ross Sea during the last 2.6 ka: From seasonal to millennial timescales. Quaternary
959 Science Reviews 237, 106299.

960 Tesi, T., Geibel, M.C., Pearce, C., Panova, E., Vonk, J.E., Karlsson, E., Salvado, J.A., Kruså,
961 M., Bröder, L., Humborg, C., Semiletov, I., Gustafsson, Ö., 2017. Carbon geochemistry of
962 plankton-dominated samples in the Laptev and East Siberian shelves: contrasts in suspended
963 particle composition. Ocean Science 13, 735-748.

964 van der Loeff, M.R., Meyer, R., Rudels, B., Rachor, E., 2002. Resuspension and particle
965 transport in the benthic nepheloid layer in and near Fram Strait in relation to faunal
966 abundances and ^{234}Th depletion. Deep Sea Research Part I: Oceanographic Research Papers
967 49, 1941-1958.

968 Viso, A.-C., Marty, J.-C., 1993. Fatty acids from 28 marine microalgae. Phytochemistry 34,
969 1521-1533.

970 Volkman, J.K., Jeffrey, S.W., Nichols, P.D., Rogers, G.I., Garland, C.D., 1989. Fatty acid and
971 lipid composition of 10 species of microalgae used in mariculture. Journal of Experimental
972 Marine Biology and Ecology 128, 219-240.

973 Wang, S.W., Budge, S.M., Gradinger, R.R., Iken, K., Wooller, M.J., 2014. Fatty acid and
974 stable isotope characteristics of sea ice and pelagic particulate organic matter in the Bering
975 Sea: tools for estimating sea ice algal contribution to Arctic food web production. Oecologia
976 174, 699-712.

977 Wassmann, P., 1991. Dynamics of primary production and sedimentation in shallow fjords
978 and polls of western Norway. Oceanography and Marine Biology Annual Review 29, 87-154.

979 Wassmann, P., Duarte, C.M., AgustÍ, S., Sejr, M.K., 2011. Footprints of climate change in the
980 Arctic marine ecosystem. Global Change Biology 17, 1235-1249.
981

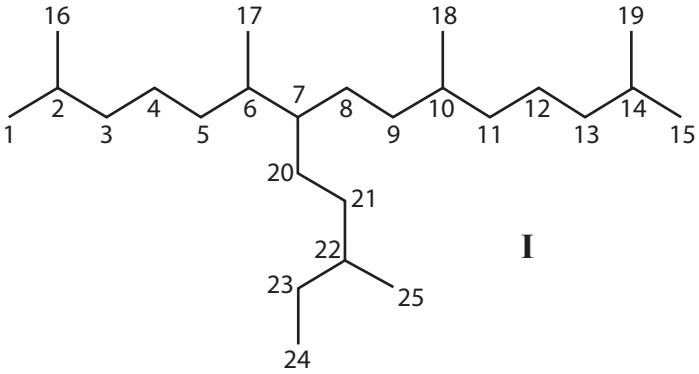

I

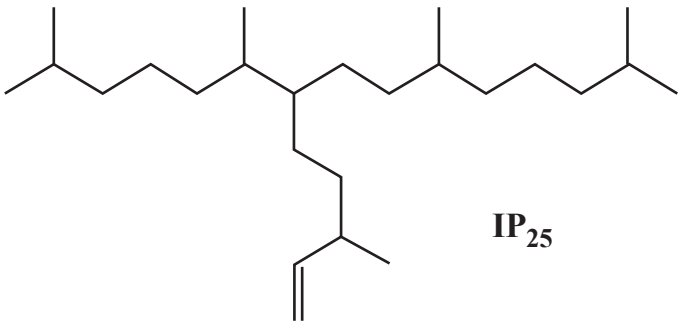

IP_{25}

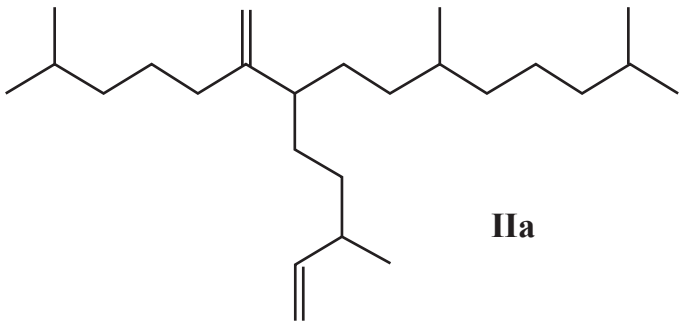

IIa

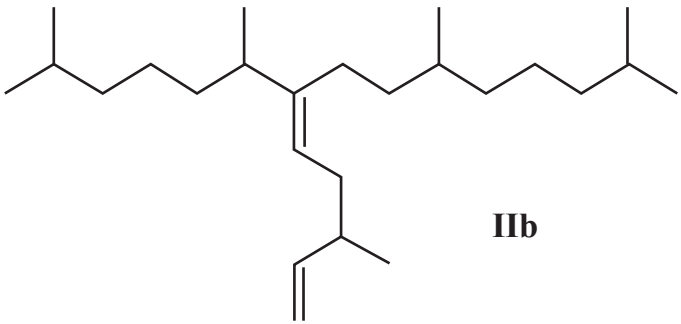

IIb

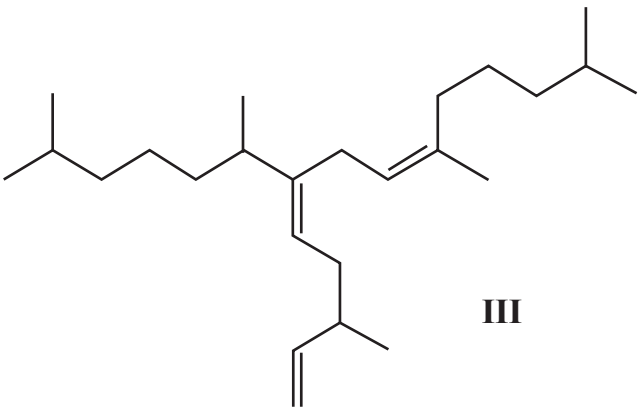

III

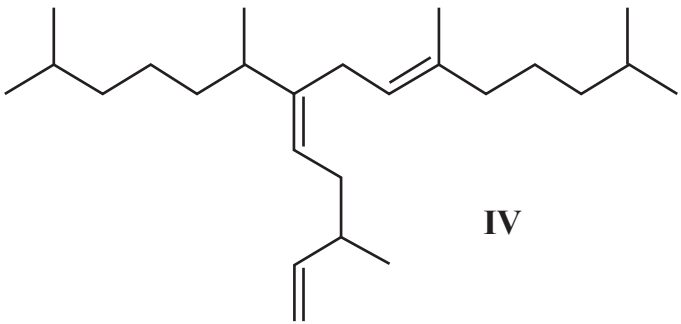

IV

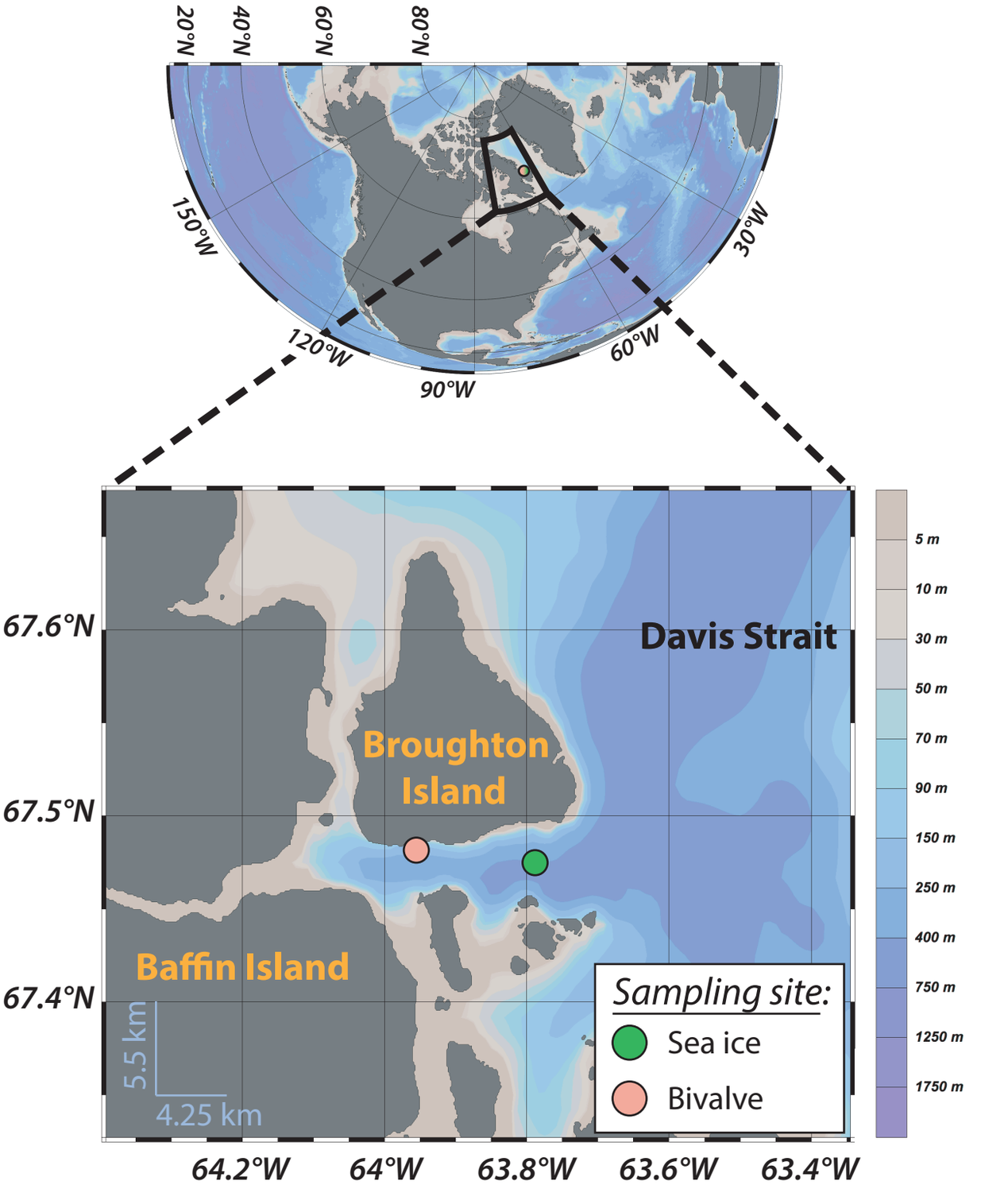
20°N
40°N
60°N
80°N
150°W
30°W
120°W
60°W
90°W
67.6°N
67.5°N
67.4°N
Davis Strait
Broughton Island
Baffin Island
5.5 km
4.25 km
64.2°W
64°W
63.8°W
63.6°W
63.4°W
Sampling site:
Sea ice
Bivalve
5 m
10 m
30 m
50 m
70 m
90 m
150 m
250 m
400 m
750 m
1250 m
1750 m

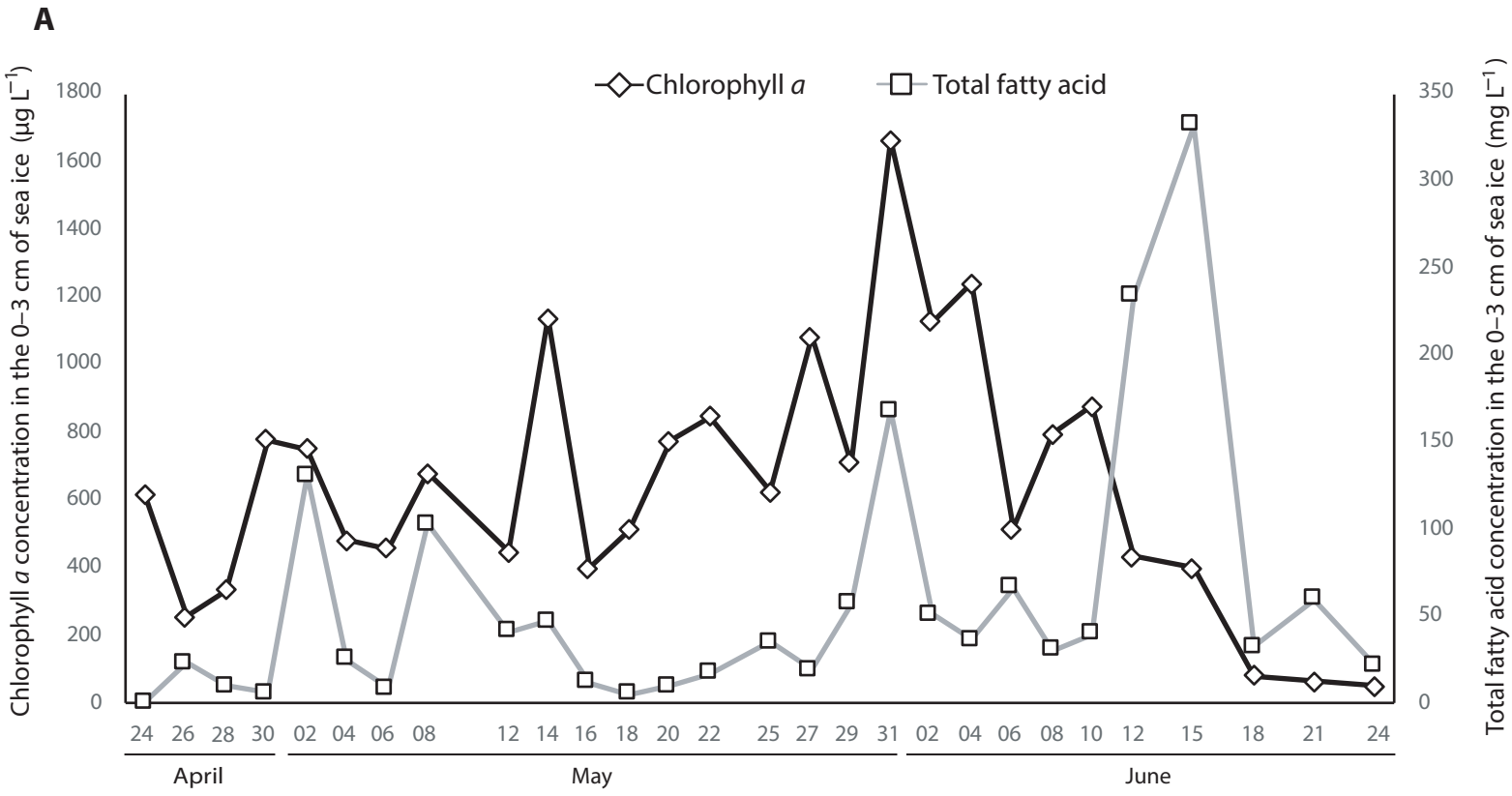
A
Chlorophyll a
Total fatty acid
Chlorophyll a concentration in the 0–3 cm of sea ice (µg L−1)
Total fatty acid concentration in the 0–3 cm of sea ice (mg L−1)
1800
1600
1400
1200
1000
800
600
400
200
0
350
300
250
200
150
100
50
0
24 26 28 30 02 04 06 08 12 14 16 18 20 22 25 27 29 31 02 04 06 08 10 12 15 18 21 24
April
May
June

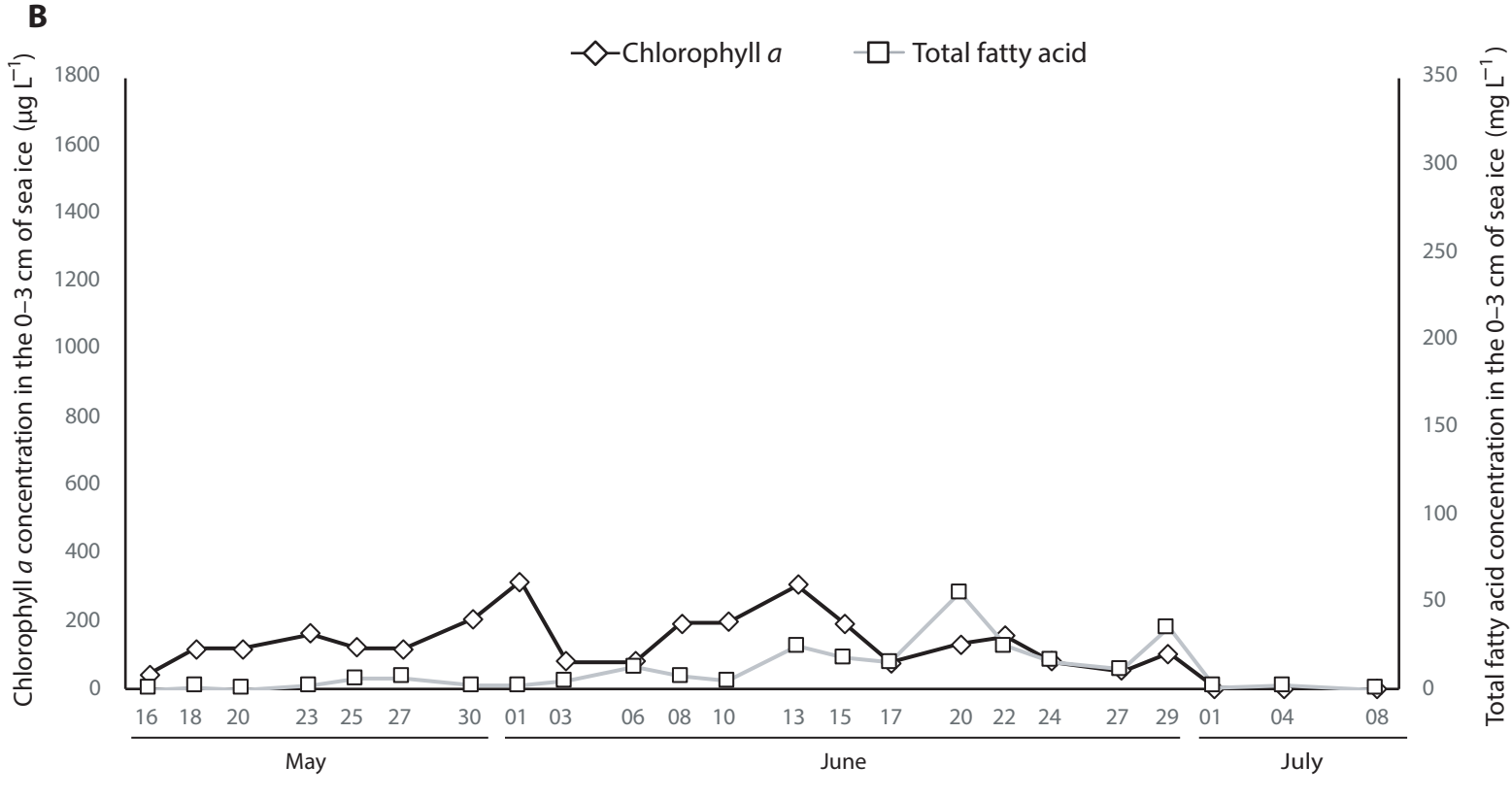
B
Chlorophyll a
Total fatty acid
Chlorophyll a concentration in the 0–3 cm of sea ice (µg L−1)
Total fatty acid concentration in the 0–3 cm of sea ice (mg L−1)
1800
1600
1400
1200
1000
800
600
400
200
0
350
300
250
200
150
100
50
0
16 18 20 23 25 27 30 01 03 06 08 10 13 15 17 20 22 24 27 29 01 04 08
May
June
July

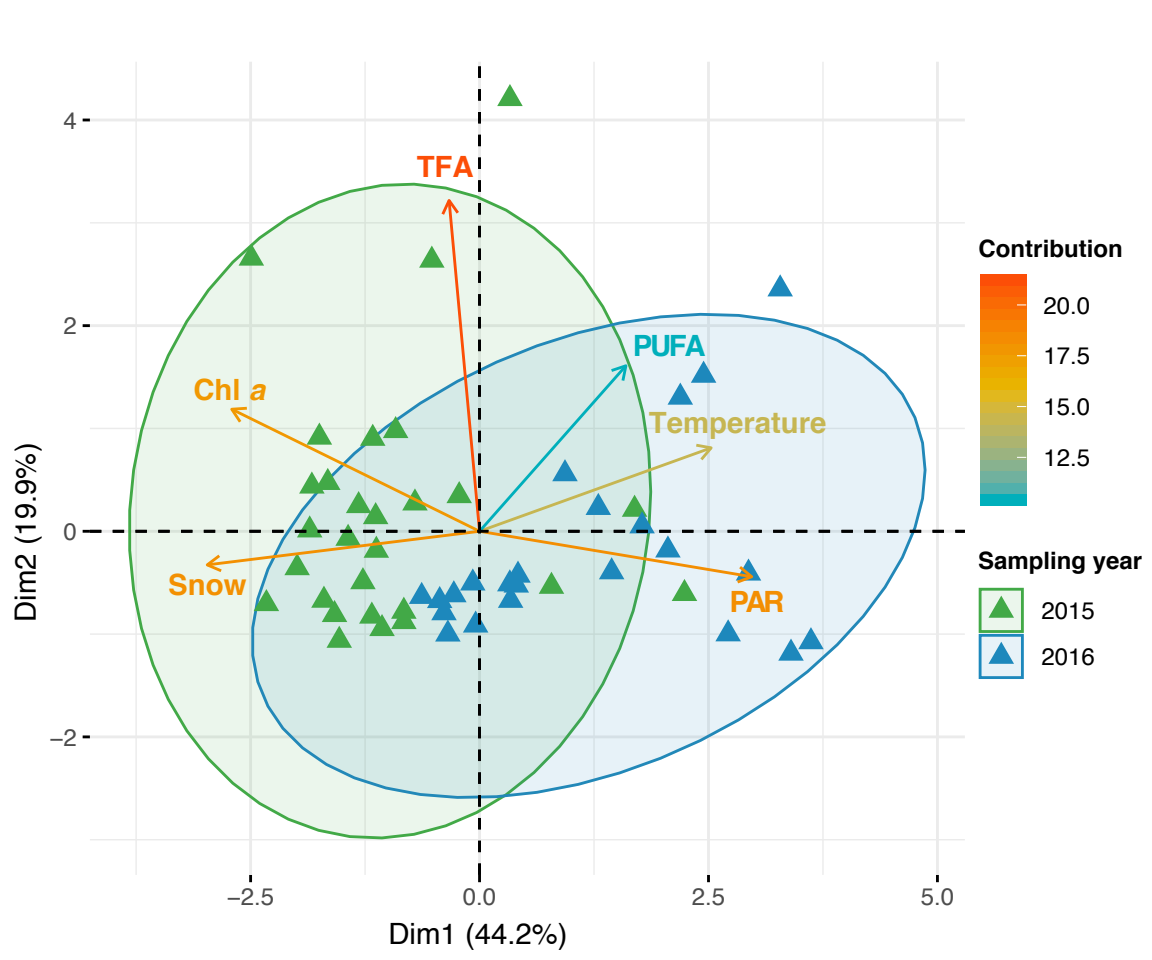
TFA
PUFA
Chl a
Temperature
Snow
PAR
Contribution
20.0
17.5
15.0
12.5
Sampling year
2015
2016
Dim2 (19.9%)
Dim1 (44.2%)
4
2
0
−2
−2.5
0.0
2.5
5.0

A

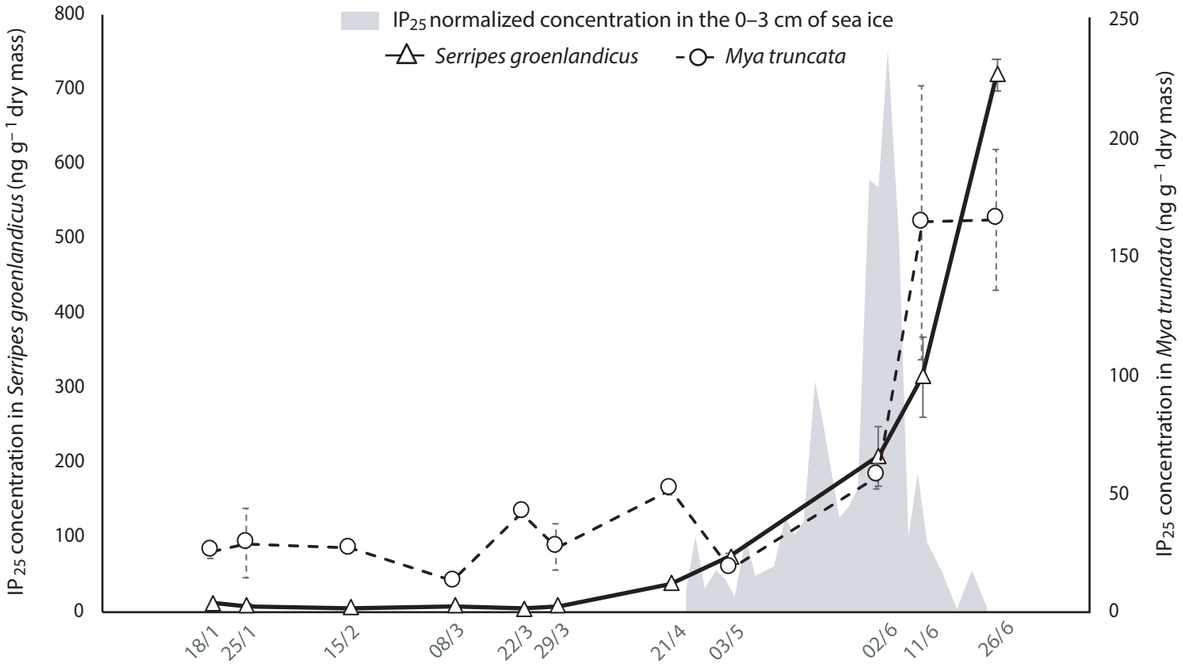
IP25 normalized concentration in the 0–3 cm of sea ice
Serripes groenlandicus
Mya truncata
IP25 concentration in Serripes groenlandicus (ng g−1 dry mass)
IP25 concentration in Mya truncata (ng g−1 dry mass)
800
700
600
500
400
300
200
100
0
250
200
150
100
50
0
18/1
25/1
15/2
08/3
22/3
29/3
21/4
03/5
02/6
11/6
26/6

B

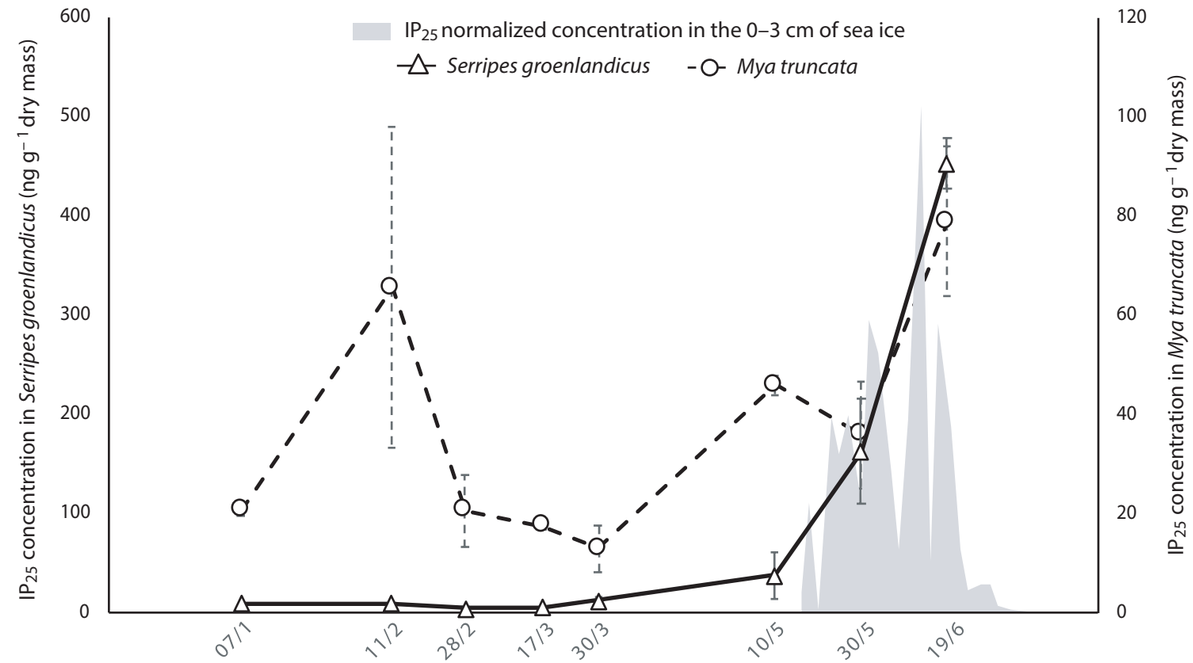
IP25 normalized concentration in the 0–3 cm of sea ice
Serripes groenlandicus
Mya truncata
IP25 concentration in Serripes groenlandicus (ng g−1 dry mass)
IP25 concentration in Mya truncata (ng g−1 dry mass)
600
500
400
300
200
100
0
120
100
80
60
40
20
0
07/1
11/2
28/2
17/3
30/3
10/5
30/5
19/6

C

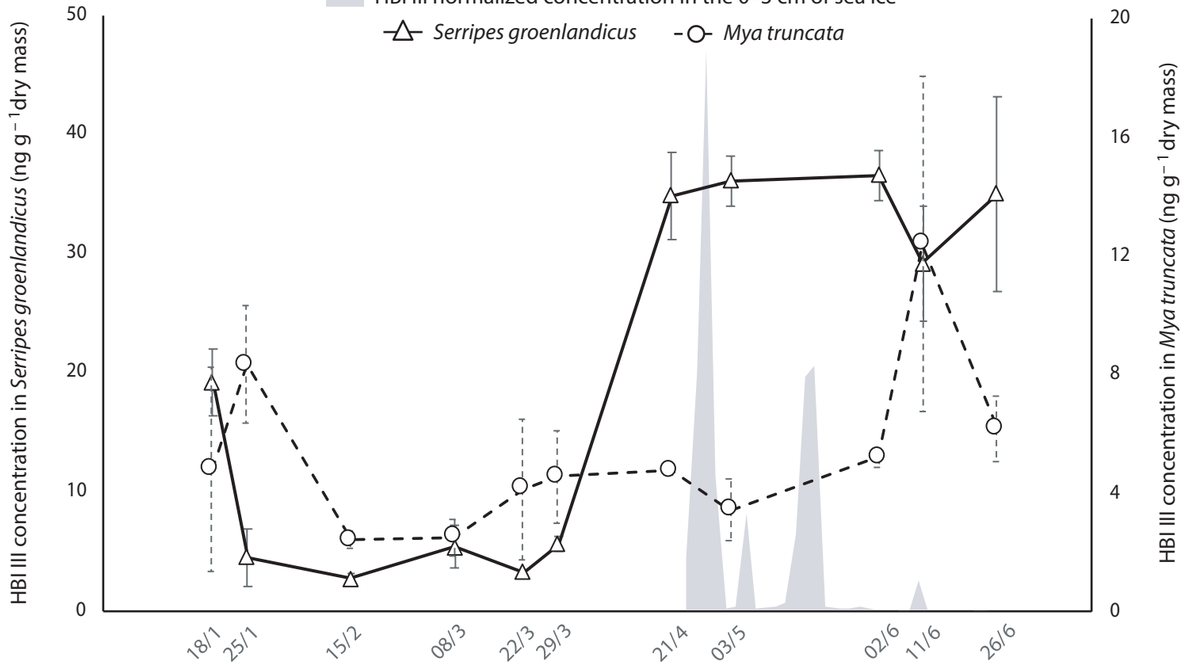
HBI III normalized concentration in the 0–3 cm of sea ice
Serripes groenlandicus
Mya truncata
HBI III concentration in Serripes groenlandicus (ng g−1dry mass)
HBI III concentration in Mya truncata (ng g−1 dry mass)
50
40
30
20
10
0
20
16
12
8
4
0
18/1
25/1
15/2
08/3
22/3
29/3
21/4
03/5
02/6
11/6
26/6

D

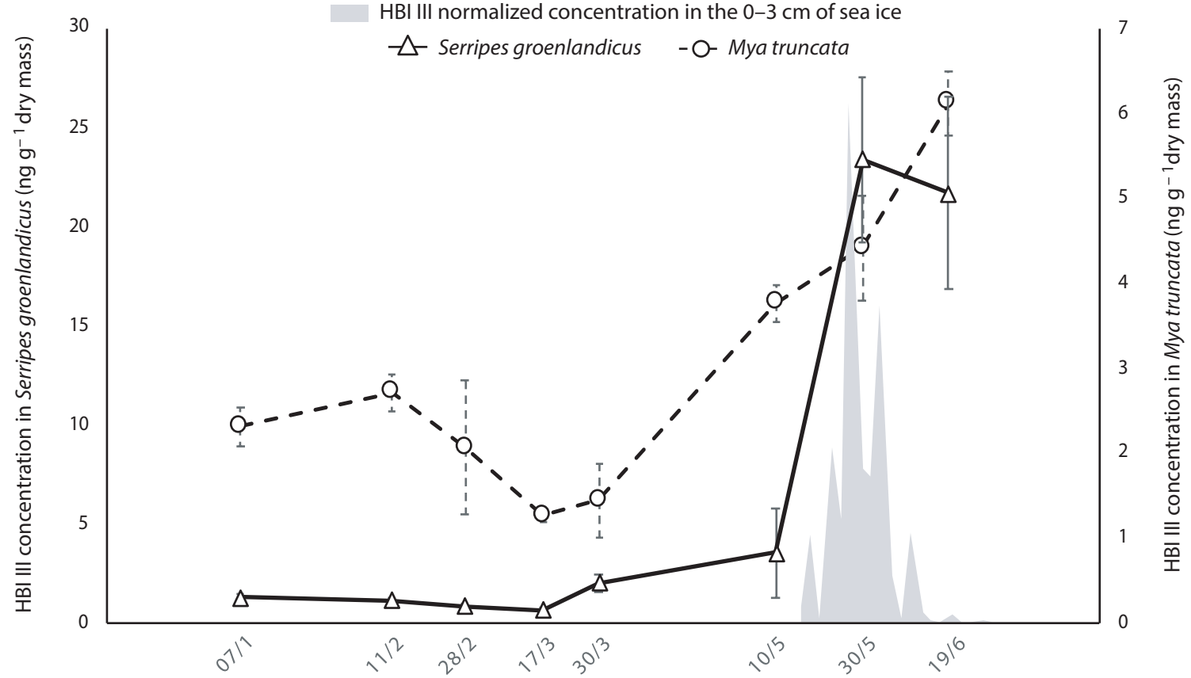
HBI III normalized concentration in the 0–3 cm of sea ice
Serripes groenlandicus
Mya truncata
HBI III concentration in Serripes groenlandicus (ng g−1 dry mass)
HBI III concentration in Mya truncata (ng g−1dry mass)
30
25
20
15
10
5
0
7
6
5
4
3
2
1
0
07/1
11/2
28/2
17/3
30/3
10/5
30/5
19/6

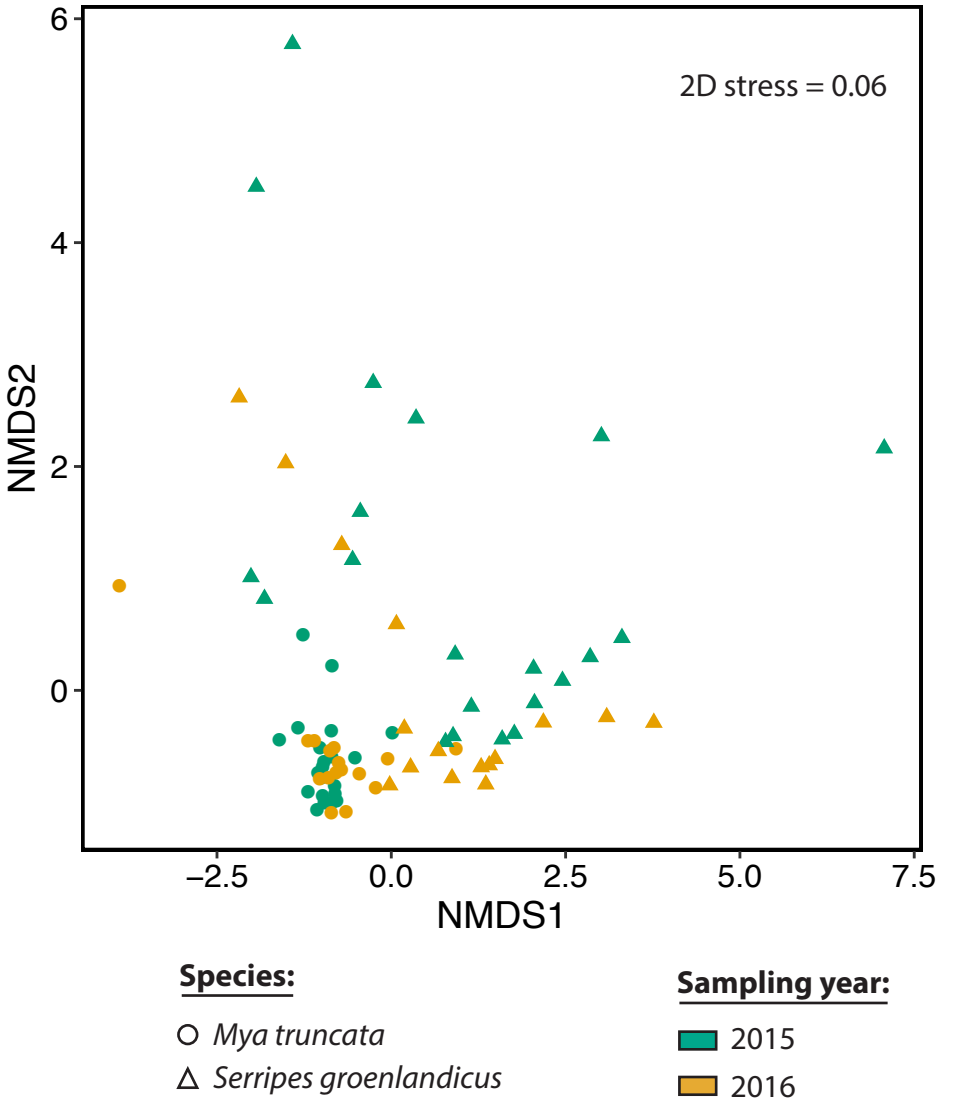
2D stress = 0.06
NMDS2
NMDS1
6
4
2
0
−2.5
0.0
2.5
5.0
7.5
Species:
Mya truncata
Serripes groenlandicus
Sampling year:
2015
2016

A

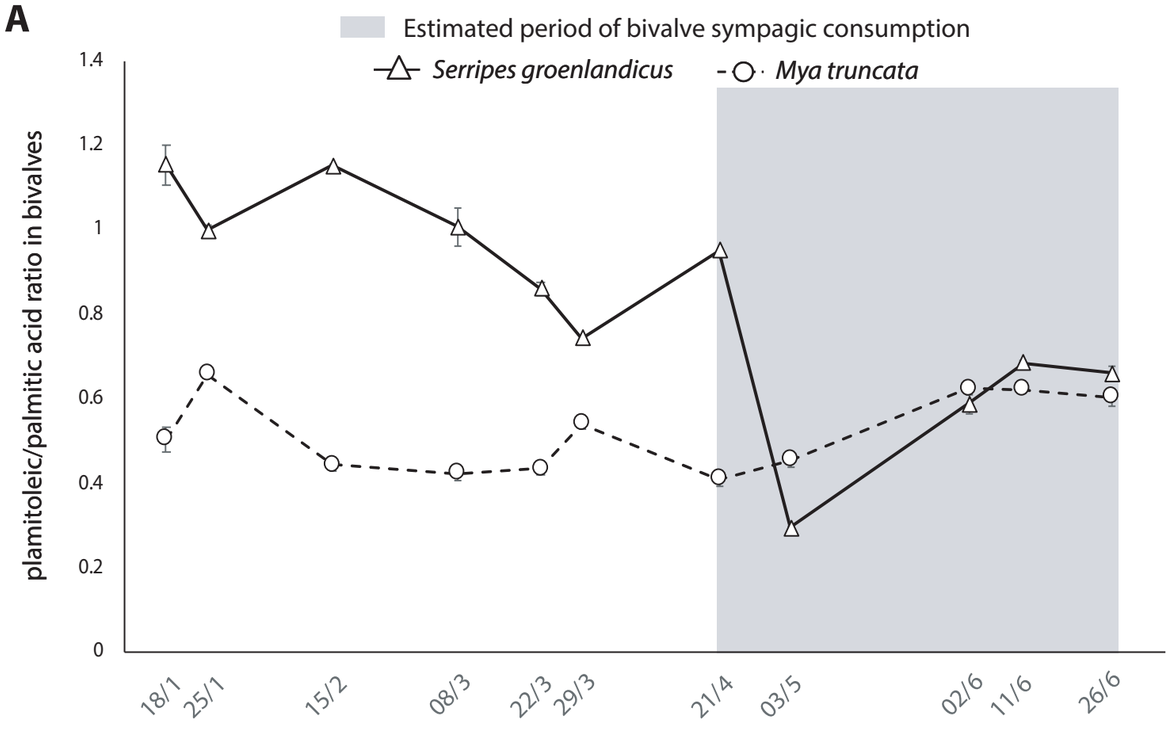
Estimated period of bivalve sympagic consumption
Serripes groenlandicus
Mya truncata
plamitoleic/palmitic acid ratio in bivalves
1.4
1.2
1
0.8
0.6
0.4
0.2
0
18/1
25/1
15/2
08/3
22/3
29/3
21/4
03/5
02/6
11/6
26/6

B

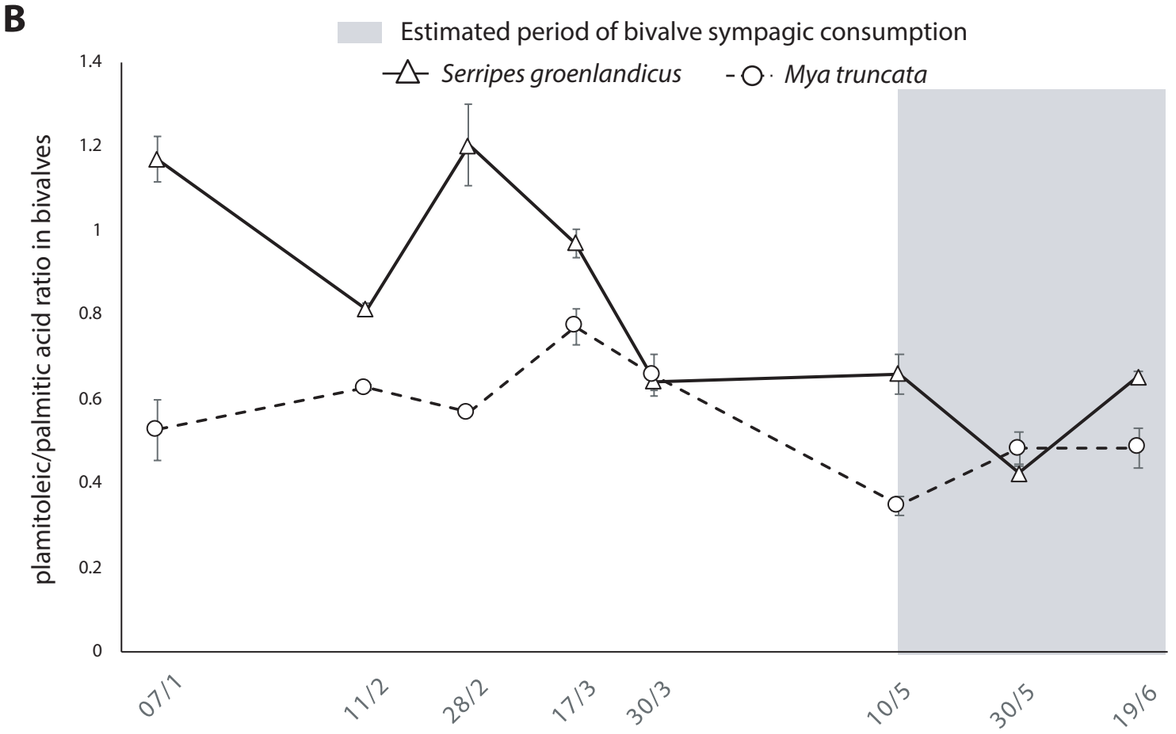
Estimated period of bivalve sympagic consumption
Serripes groenlandicus
Mya truncata
plamitoleic/palmitic acid ratio in bivalves
1.4
1.2
1
0.8
0.6
0.4
0.2
0
07/1
11/2
28/2
17/3
30/3
10/5
30/5
19/6

C

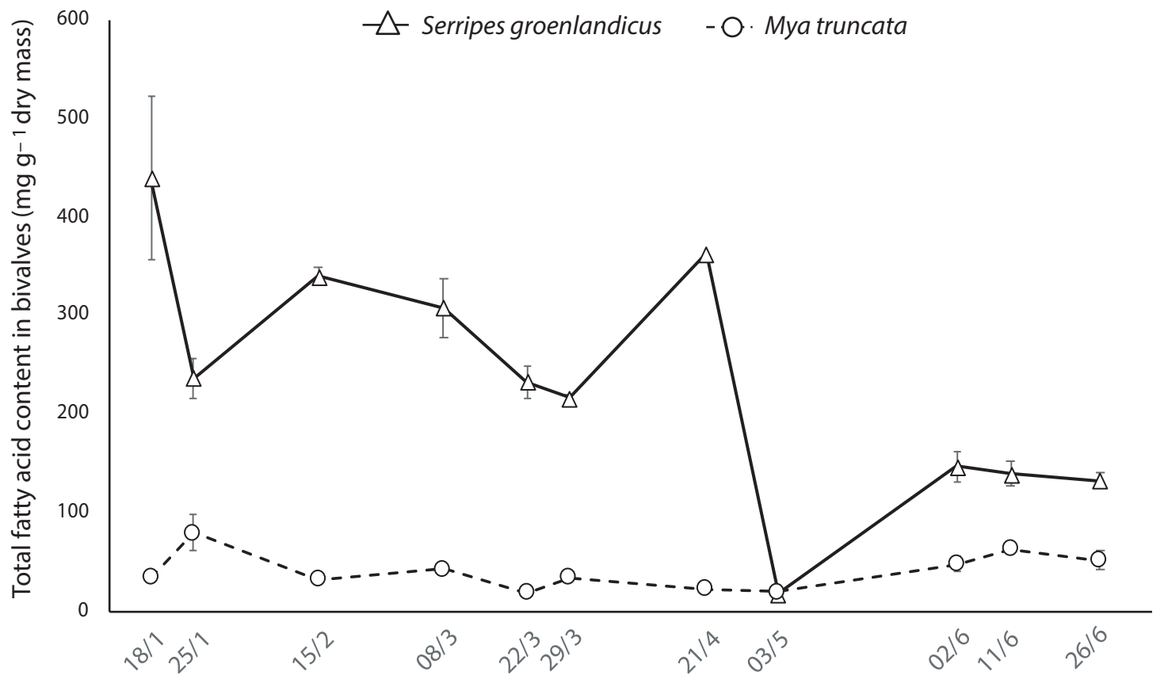
Serripes groenlandicus
Mya truncata
Total fatty acid content in bivalves (mg g⁻¹ dry mass)
600
500
400
300
200
100
0
18/1
25/1
15/2
08/3
22/3
29/3
21/4
03/5
02/6
11/6
26/6

D

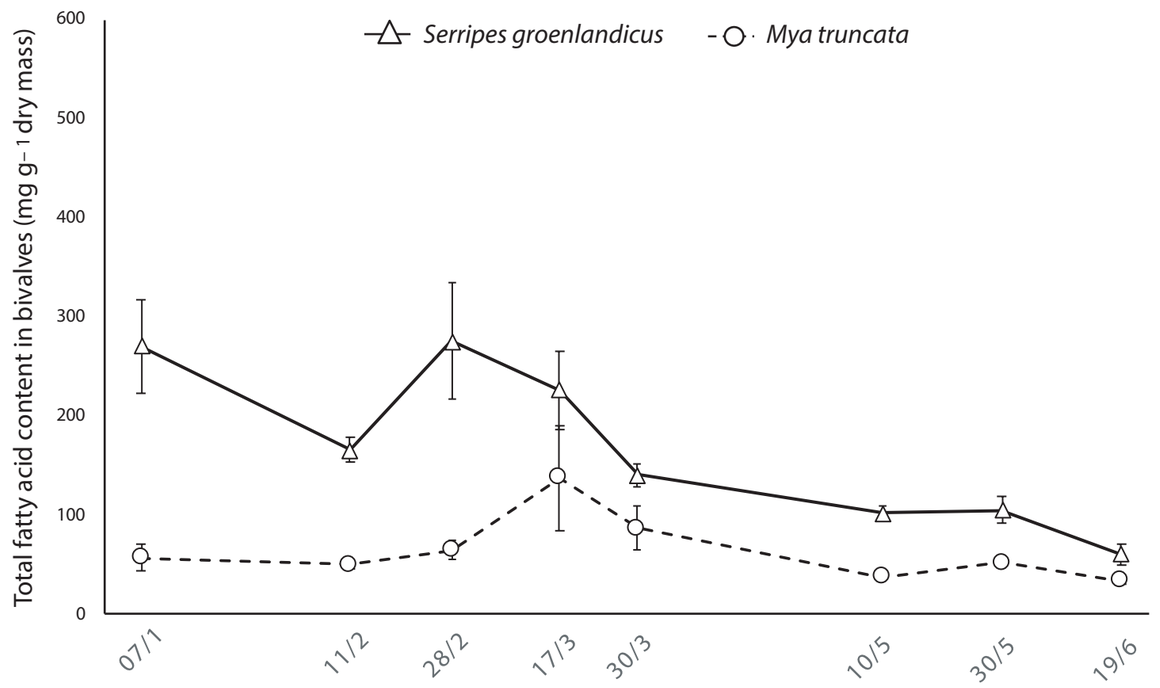
Serripes groenlandicus
Mya truncata
Total fatty acid content in bivalves (mg g⁻¹ dry mass)
600
500
400
300
200
100
0
07/1
11/2
28/2
17/3
30/3
10/5
30/5
19/6

E

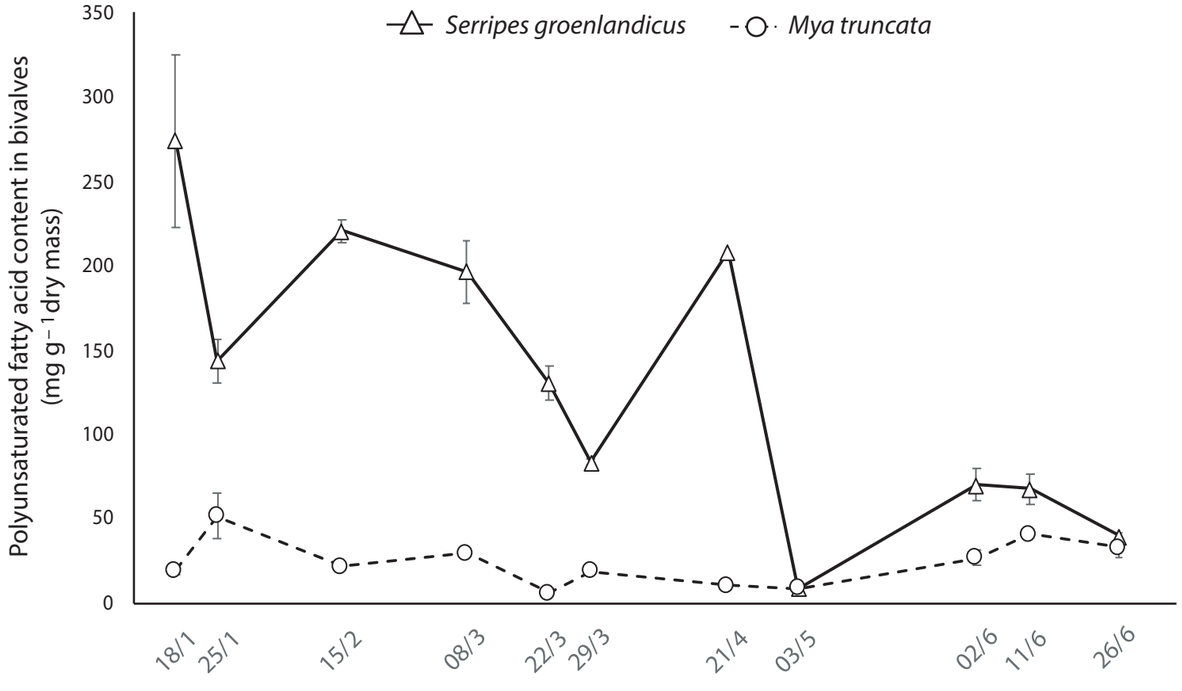
Serripes groenlandicus
Mya truncata
Polyunsaturated fatty acid content in bivalves (mg g⁻¹ dry mass)
350
300
250
200
150
100
50
0
18/1
25/1
15/2
08/3
22/3
29/3
21/4
03/5
02/6
11/6
26/6

F

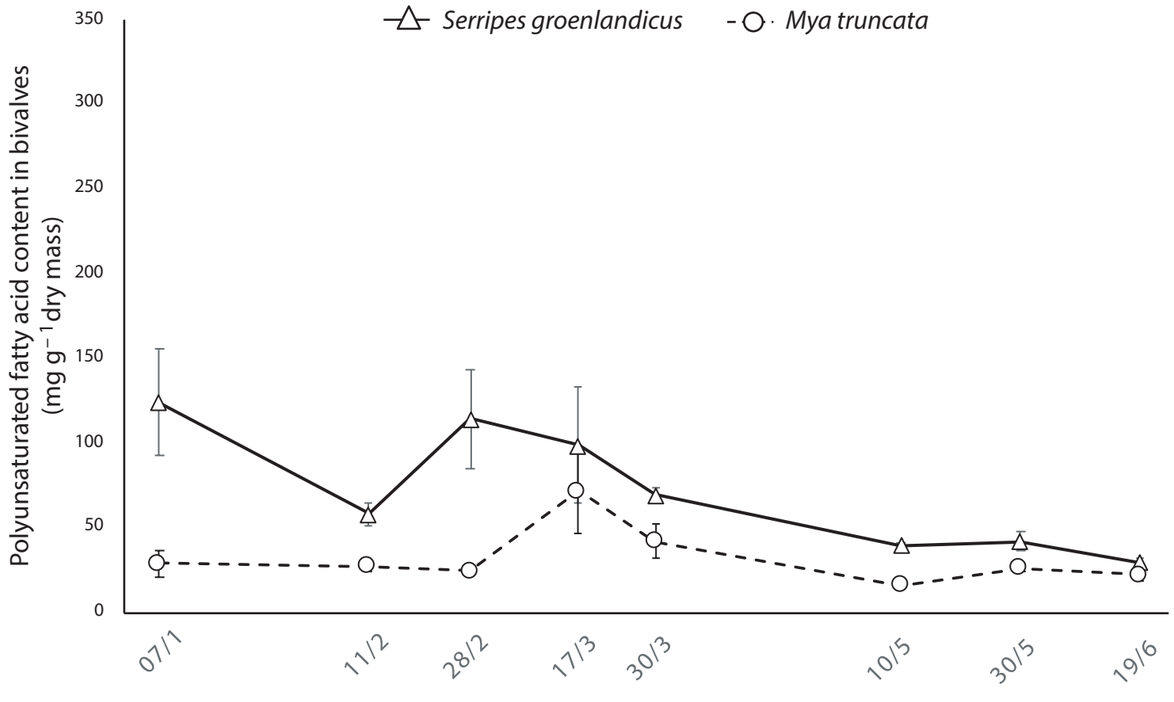
Serripes groenlandicus
Mya truncata
Polyunsaturated fatty acid content in bivalves (mg g⁻¹ dry mass)
350
300
250
200
150
100
50
0
07/1
11/2
28/2
17/3
30/3
10/5
30/5
19/6

Table 1: Mean fatty acid composition, expressed as mass % of total fatty acids (TFA), of POM collected in the 0–3 cm of sea ice in Davis strait between 24 April to 24 June 2015 and, 16 May to 8 July 2016. Fatty acids above > 3% in at least one of the sea ice sampling investigated were included. TFA = total fatty acids expressed in mg L^{-1}; SFA = saturated fatty acid; MUFA = monounsaturated fatty acid; PUFA = polyunsaturated fatty acid. Values are mean (SE).

Fatty acid	**Sea ice sampling year**	
	2015	2016
14:00	4.7 (0.4)	4.2 (0.3)
16:00	26.1 (1.9)	30.8 (2.8)
∑SFA	30.7 (1.9)	35.0 (2.8)
16:1ω7	68.9 (2.0)	53.6 (3.2)
18:1ω9	5.4 (0.1)	0.3 (0.1)
∑MUFA	68.9 (2.0)	53.6 (3.2)
EPA	0.5 (0.3)	10.3 (1.7)
DHA	0.0 (0.0)	1.2 (0.3)
∑PUFA	0.4 (0.3)	11.4 (1.9)
TFA[a]	57.9 (14.0)	11.0 (2.7)

[a] Expressed in mg L^{-1}

Table 2: Correlation coefficients between chlorophyll *a* (Chl *a*) and HBI biomarkers in sea ice POM, *Serripes groenlandicus* and *Mya truncata* collected in 2015 and 2016 in Davis Strait (**Figure 2**).

Sample type	Factor	Chl *a*	IP_{25}	HBI IIa	HBI IIb	HBI III
Sea ice POM	Chl *a*	1	–[b]	–	–	–
(n = 51)	IP_{25}	0.58*[a]	1	–	–	–
	HBI IIa	0.61*	0.92*	1	–	–
	HBI IIb	n/a[c]	0.27	0.34	1	–
	HBI III	0.39*	0.32	0.39*	0.88*	1
	HBI IV	0.45*	0.41*	0.47*	0.87*	0.94*
Serripes groenlandicus	IP_{25}	n/a	1	–	–	–
(n = 38)	HBI IIa	n/a	0.99*	1	–	–
	HBI IIb	n/a	0.74*	0.79*	1	–
	HBI III	n/a	0.62*	0.64*	0.72*	1
	HBI IV	n/a	0.69*	0.72*	0.70*	0.87*
Mya truncata	IP_{25}	n/a	1	–	–	–
(n = 38)	HBI IIa	n/a	0.44*	1	–	–
	HBI IIb	n/a	0.60*	0.39*	1	–
	HBI III	n/a	0.71*	0.15	0.60*	1
	HBI IV	n/a	0.37*	0.71*	0.70*	0.21*

[a]Asterisk indicates significant correlation: $p < 0.01$.
[b]Repetition of value.
[c]Not applicable.

Table 3: Mean fatty acid composition, expressed as mass % of total fatty acids (TFA), of (A) *Serripes groenlandicus* and (B) *Mya truncata* collected in Davis strait between January and June 2015 and between January and June 2016. Fatty acids above >3% in at least one of the bivalve sampling investigated were included. TFA = total fatty acids expressed in mg g^{-1} dry mass; SFA = saturated fatty acid; MUFA = monounsaturated fatty acid; PUFA = polyunsaturated fatty acid. Values are mean (SE).

Fatty acid	***Mya truncata* sampling year**		***Serripes groenlandicus* sampling year**	
	2015	2016	2015	2016
14:00	1.9 (0.3)	2.7 (0.5)	5.7 (0.4)	6.9 (0.6)
16:00	23.8 (2.5)	30.2 (3.4)	20.7 (1.0)	25.6 (2.7)
∑SFA	25.7 (2.8)	32.9 (3.8)	26.4 (1.4)	32.5 (3.3)
16:1ω7	12.0 (1.7)	16.5 (3.0)	15.8 (1.3)	20.0 (2.9)
18:1ω9	3.3 (0.5)	3.8 (0.7)	4.3 (0.3)	5.3 (0.8)
∑MUFA	15.3 (2.2)	20.3 (3.7)	20.1 (1.6)	25.3 (3.7)
EPA	42.7 (5.9)	37.4 (6.0)	44.9(4.1)	35.3 (5.9)
DHA	16.2 (1.4)	9.3 (0.8)	8.5 (0.5)	6.8 (1.0)
∑PUFA	58.9 (7.2)	46.7 (6.8)	53.5 (4.6)	42.2 (6.9)
TFA[a]	40.1 (5.0)	54.6 (11.0)	233.5 (19.7)	167.6 (25.2)

[a] Expressed in mg L^{-1}